DOKUZ EYLÜL UNIVERSITY
GRADUATE SCHOOL OF NATURAL AND APPLIED SCIENCES

PRODUCTION AND CHARACTERIZATION OF CaP COATINGS ON METALLIC IMPLANTS BY ELECTROPHORETIC DEPOSITION

by
Utku TİRİÇ

October, 2019
İZMİR

PRODUCTION AND CHARACTERIZATION OF CaP COATINGS ON METALLIC IMPLANTS BY ELECTROPHORETIC DEPOSITION

A Thesis Submitted to the
Graduate School of Natural and Applied Sciences of Dokuz Eylül University
In Partial Fulfillment of the Requirements for the Degree of Master of Science
in Metallurgical and Materials Engineering Program

by
Utku TİRİÇ

October, 2019
İZMİR

M.Sc THESIS EXAMINATION RESULT FORM

We have read the thesis entitled **"PRODUCTION AND CHARACTERIZATION OF CaP COATINGS ON METALLIC IMPLANTS BY ELECTROPHORETIC DEPOSITION"** completed by **UTKU TİRİÇ** under supervision of **ASSIST. PROF. DR. IŞIL BİRLİK** and we certify that in our opinion it is fully adequate, in scope and in quality, as a thesis for the degree of Master of Science.

Assist. Prof.Dr. Işıl BİRLİK

Supervisor

Assist. Prof. Dr. Funda AK AZEM

(Jury Member)

Assist. Prof. Dr. Onur ERTUĞRUL

(Jury Member)

~~Prof. Dr. Kadriye~~ ERTEKİN

Director
Graduate School of Natural and Applied Sciences

ACKNOWLEDGMENTS

Firstly, I would like to express to my deep and sincere gratitude to my advisor, Assist Prof. Dr. Işıl BİRLİK, for her excellent guidance, patient supervision and continuous support thought the preparation of this study.

I thank to my co-advisor Assist. Prof. Dr. Funda AK AZEM for her assistance and guidance during my working.

I warmly express my special thanks to my co-workers, Tülay KOÇ DELİCE and Bensu BAKIN for their supports, helps, patience and friendships.

Finally, I would like to express my deep and sincere thanks to my family for their love, encouragement and endless patience during my education.

Utku TİRİÇ

PRODUCTION AND CHARACTERIZATION OF CaP COATINGS ON METALLIC IMPLANTS BY ELECTROPHORETIC DEPOSITION

ABSTRACT

Titanium and its alloys are choosed metals for load resistant biomaterials and the features of Titanium is significant variable in medical form. Surface alteration are broadly used to regulate the features of titanium surface to the special needs of the medicinal operations.

Several Calcium Phosphate coating method has been used as plasma spray, biomimetic deposition, sol-gel, electrochemical deposition and electrophoretic deposition. The electrophoretic deposition coating technique has a different of advantages for instance process at low temperature, ability to coati on spongy or complex shape of implant, low cost and easiness of coating dimension control. However, agglomeration of Calcium Phosphate powder in suspension adversely affect the morphology of the coating.

In this study surface modification was performed on Titanium alloy plates (substrates) by electrophoretic deposition (EPD) method. The aim of the study is to research the effect of type of dispersant on structure and morphology of produced Calcium Phosphate coatings. The size distribution and zeta potential of the Calcium Phosphate particles in suspension were determined by a zeta-sizer. Phase analysis, chemical characterizations and morphological characterizations of the Calcium phosphate depositions were determined by using X-ray Diffraction (XRD), Fourier Transform Infrared Spectroscopy (FTIR) and Scanning Electron Microscope (SEM), respectively. The corrosion behavior of the CaP coatings were determined by a electrochemical characterization method.

Keywords: Calcium phosphate coatings, electrophoretic deposition, dispersant, diethanolamine, Titanium, Ti6Al4V alloy

METALİK İMPLANTLAR ÜZERİNE CaP KAPLAMALARIN ELEKTROFORETİK ÇÖKTÜRME YÖNTEMİ İLE ÜRETİMİ VE KARAKTERİZASYONU

ÖZ

Titanyum ve Titanyum esaslı alaşımlar yük taşıyıcı implant uygulamalarında tercih edilmektedir ve titanyumun yüzey özellikleri implant tasarımında kullanılan önemli değişkenlerden biridir. Titanyumun yüzey modifikasyonu, medikal uygulamalarda spesifik ihtiyaçları karşılamak amacıyla yaygın bir şekilde kullanılmaktadır. Bu çalışmada Titanyum alaşımı altlıklara yüzey modifikasyon işlemi elektroforetik biriktirme yöntemi ile uygulanmıştır. Kalsiyum fosfat kaplamalar için, plazma sprey, biyomimetik çöktürme, sol-jel, elektrokimyasal çöktürme ve elektoforetik biriktirme gibi birçok yöntem kullanılmıştır. Elektroforetik biriktirme düşük işlem sıcaklığı, gözenekli yada karmaşık yapıdaki altlıklara çöktürme imkanı sağlaması, düşük maliyeti ve kaplama kalınlığının kolay kontrolü gibi birçok avantaja sahiptir. Buna karşın Kalsiyum fosfat tozlarının süspansiyon içerisinde aglomera olması, elektroforetik çöktürme yönteminde kullanılan süspansiyonun özelliklerini ve kaplamaların morfolojisini olumsuz etkilemektedir.

Çalışmanın amacı dispersant türüne bağlı olarak üretilmiş olan kalsiyum fosfat kaplamaların yapısal ve morfolojik özelliklerinin incelenmesidir. Kalsiyum fosfat partiküllerin tane boyut dağılmı ve zeta potansiyeli değerleri zeta-sizer cihazıyla belirlenmiştir. Kalsiyum fosfat kaplamaların faz analizleri, kimyasal ve morfolojik karakterizasyonları ise sırasıyla X-ışını difraksiyonu, fourier kızılötesi spektroskopisi ve taramalı elektron mikroskobu kullanarak belirlenmiştir. Kalsiyum fosfat kaplamaların korozyon davranışları elektrokimyasal teknikler kullanılarak beirlenmiştir.

Anahtar kelimeler: Kalsiyum fosfat kaplamalar, elektroforetik çöktürme, dispersant, dietanolamin, Titanyum, Ti6Al4V alaşım

CONTENTS

Page

LIST OF FIGURES

Page

LIST OF TABLES

Page

CHAPTER ONE
INTRODUCTION

The biomaterial is used to change or repair function of tissue. The utilize of metals to fix the body has been reported for centuries (Agrawal, 1998). Generally, these biomaterials can be sperated the categories: metals, polymers, ceramics, and composites (Davis, 2003). Titanium and its alloys were identified by William Gregor in England in the year 1791 and named by Martin Heinrich Klaproth for the Titans of Greek mythology (Levitus & Boyer, 1994). Titanium and its alloys are boradly utilized as biomaterials because of their attractive mechanical features and chemical steadily in physiological environment. Regardless, the complication is to bond with living body tissue (Huang et al., 2008).

Formation of calcium phosphate on titanium biomaterials have been researched for decades. Some scientist has proved that thin calcium phosphate films can efficiently create connection between the biomaterials and host bone (Cheng et al., 2013). Titanium biomaterials are frequently deposited with hydroxyapatite ($Ca_{10}(PO_4)_6(OH)_2$), a bioceramic which resembles the mineral constituents of bones (Kwok, Wong, Cheng, & Man, 2009). Yet the mechanical resistance of Hydroxyapatite (HAP) is too low to be choosed in load supporting operations. Accordingly, HAP coatings were deposited on metallic implants to increase the biocompatibility feature (Bir et al., 2012).

There are various method which has been used to achieve hydroxyapatite formations on metallic biomaterials such as sol-gel processing (Azem, Eroglu, & Cakir, 2011), plasma spray (Yang & Yang, 2013), electrophoretic deposition (EPD) (Mondragon-Cortez & Vargas-Gutierrez, 2004), pulsed laser deposition (PLD) (Zeng & Lacefield, 2000), biomimetic coating (Habibovic, Barrere, Van Blitterswijk, de Groot, & Layrolle, 2002), and magnetron sputtering (Long et al., 2002). In the EPD method is not only by its simple apply to different materials but also by its simplicity; EPD is a low cost technique generally needs to simple tool (Wei, Ruys, Milthorpe, & Sorrell, 2005). The electrophoretic deposition of the particles depend extremely, on

the suspension and process related parameters. Many important parameters related to the suspension are to be considered in the EPD, these are types of liquid mediums (solvent), particle size, concentration and dispersant (Besra & Liu, 2007). At the same time many important process parameters effects to EPD, these are applied voltage, time, conductivity of the substrate, deposition time (Wang, Leu, & Hon, 2004).

1.1 Aim and Objective of The Study

The fundamental purpose of this study is to research the effect of dispersant on morphological properties of CaP coatings prepared by electrophoretic deposition in the CaP based suspension. Besides, the effect of different surface modifications applied to substrate was also examined. The content of the study includes:

1. Preparation of Ti6Al4V substrates
2. Preparation of suspensions for deposition of CaP on Ti6A4V substrates.
3. Investigation of concentration of dispersant effect in suspension.
4. Analysis of the morphological features and corrosion behavior of the coatings.
5. Characterization of CaP coatings.
6. Discussion of effect of various concentration of dspersant mechanism of the coatings morphology by supporting with literature and analyzing results.

The structure of thesis consists of six chapter which are summarized below:

Chapter 1 is a introduction and describes briefly aim of this thesis.

Chapter 2 is a literature review, including classification and properties of biomaterials. Also, surface modification of the biomaterials spesifically EPD process which is used in this study is described in this chapter.

Chapter 3 is a literature review, including production methods of CaP coatings.

Chapter 4 describes experimental studies including experimental setup, suspension preparation, substrate preparation, surface modification of Ti6Al4V substrates, coating of substrates and characterization technique of suspensions and coatings.

Chapter 5 is the results and discussion part. The mechanism of the dispersant is discussed with regard to morphology of coatings.

Chapter 6 includes the remarkable conclusions of this study.

CHAPTER TWO
BIOMATERIALS

2.1 Introduction

Studies in recent times, there have been escalationing persistence of materials utilizations in biomedical operations. In spite of the explanation of "biomaterials" can have encountered various clarifications both in material science and clinical application (Donglu, 2005). Biomaterial is defined as a man-made material, which is embedded to supplant tissue for satisfying natural performances of the living body (Li, Park, & Bronzino, 2003). The biomedical implants are placed in various parts of the living tissue as artificial valves in the heart, stents cardiovascular system; eye lens replacement, artificial stapes in ear for sense organs; reinstatement biomaterials in shoulders, knees, hips, elbows, ears and orthodental structures for the skeleton system (Ramakrishna, Mayer, Wintermantel, & Leong, 2001).

The achivement of an implant is decidedly related with biocompatibility of the implant. Biocompatibility could be describe as, the capability of a biomaterial with a convenient host reaction at clinical specific operation. Accordingly the tissue response situtations, the biocompatibility of biomaterials is classified within three categories by (Heimke & Stock, 1984), which are biotoleranceness, bioinertness and bioactiveness. The term “biotolerant” identify osteogenesis (bone evolution with undirect connect to the biomedical implant); “bioinert”, the contact osteogenesis (bone evolution with forthright contact to the material), and “bioactive”, the holding osteogenesis (bone evolution with biological connecting to the biomedical implant) (Heimke & Stock, 1984). The classification of interactions between implants and hard tissue shown in Table 2.1.

Table 2.1 Classification interaction between tissue and implants

Biocompatible	The capability of coexistence with living tissues without causing harm
Biotolerant	Seperated from bone tissue by a layer of fibrous tissue
Bioinert	No chemical reactions occur between the biomaterial and tissue
Bioactive	The collagen and mineral phase of the bone is deposited straight on the implant surface

The biological reaction and consecutive performance of a biomaterial is altered by the substrate features. Consequently, surface alterations of materials stand for encouraging routes to engineer biofunctionality at the material–tissue interface to regulate biological returns without adjusting material bulk features. Innumerous technologies have been advanced to design (1) physicochemical alteration including modifications to the chemicals on the surface, and (2) coatings comprising of a various biomaterial from the inherent support, including not mobilized biomolecules. These situations hold prodigious promise to increase implant function in medicine (Agarwal & García, 2019).

Most synthetic biomaterial utilized for biomedical applications are accepted materials acquaintant to the scientist. Generally these biomaterials can be branched into four groups. Classifications of materials: ceramics, metals, polymers and composites are used for such clinical applications shown in Table 2.2 (Davis, 2003).

Table 2.2 Medical and dental materials and their clinical applications

Classes	Materials	Principal applications
Metals	Stainless steel (316L)	Fracture fixation, stents, surgical instruments
	CP-Ti, Ti-Al-V, Ti-Al-Nb,Ti, Ti-13Nb-13Zr	Bone and joint substituent fracture fixation, dental implants, pacemaker encapsulation
	CoCrMo, CrNiCrMo	Bone substituent, Heart valves, dental implants
	Nickel-Titanium	Bone plates, vessel stents, dental wires
	Gold alloys	Dental reclamations
	Silver	Antibacterial agents
	Platinum and Platinum-Iridium	Electrodes
	Mercury-silver amalgam	Dental operations
Ceramics and Glasses	Al_2O_3	Joint substituent, dental implants
	ZrO_2	Joint substituent
	CaP	Bone repair, surface coating on metals
	Bioactive glass	Bone substituent
	Hard ceramic (Porcelain)	Dental reinstatement
	Carbon based ceramics	Heart valves, dental implants
Polymers	Polyethlene	Joint substituent
	PP	Sutures
	Polyethylene	Sutures, vascular supports
	Polyamides	Sutures
	Polytetrafluoroethylene	Soft tissue augmentation vascular prostheses
	Polyesters	Vascular tools, drug-delivery applications
	Polyurethanes	Blood-contacting equipments
	Polyvinyl chloride	Tubing
	Polymethyl methacrylate (PMMA)	Dental reclamations, ocular lenses, bone cements
	Silicones	Soft-tissue substituent, ophthalmology
	Hydrogels	Ophthalmology, drug deliver operations
Composite	BIS-GMA-silica and PMMA-glass	Dental reclamations

Some of advantages and disadvantages of four groups of synthetic materials utilized for implantation shown in Table 2.3 (Park & Lakes, 2007).

Table 2.3 Advantages and disadvantages of synthetic biomaterials

Materials	Advantages	Disadvantages
Metals	Strong Tough Ductile	May corrode Dense Difficult to make
Ceramics	Very bio-compatible	Brittle Not resilient Weak in tension
Polymers	Resilient Easy to produce	Weak Deforms with time
Composites	High strength Tailor-made	Difficult to produce

2.2 Metallic Biomaterials

Utilization of metallic biomaterials for biomedical aplications can be traced back to the 19th century, leading up to the period when the metal sector started to grow during the Industrial Revolution (Park & Lakes, 2007). Although many number of metals or alloys produce in factory, just a couple are biocompatible and capable of long term achieve as an biomaterial. In order to serve harmlessly and properly for a long time without elimination, a metallic biomaterial should possess the following fundamental properties, but not limited to; attractive biocompatibility (non-toxic), strength corrosion resistance, suitable mechanic features, strength wear resistance and osseo-integration.

The design and selection of a metallic implant rely on its special medical utilization. Metallic alloys are used earnestly in equipments such as catheter wires, orthodontic dental wires, vascular vessel stents and medical implants. Some metals can be utilized for passively for hard bone tissue surrogate like hip and patella joint, bone plates, screws and because of their attractive mechanical features and corrosion resistance used as dental implants.

2.2.1 Stainless Steels

The recommended stainless steel for biomaterial use is shown in Table 2.2. The early stainless steels used for implant manufacturing was the type 302. Type 302 (18-8 old classification) is more stable and has better corrosion behavior than vanadium content steel. Type 302 was advertised which contains a little percentage of Molybdenum to increase the corrosion behavior in salty solution which prepared from chloride. This metallic alloy known as 316 stainless steel. Carbon content of 316 stainless steel was decreased from 0.08 to maximal amount of 0.03% for higher corrosion behaviour in salty water. So this alloy known as 316L stainless steel.

316L austenitic stainless steel (ASTM F138/139) may occur corrosioın inside the body under specific conditions in very high stressed and devoid of oxygen zone, for instance under the screws of the bone crack fixing plate. To increase of, wear resistance, corrosion resistivity, and fatigue resistivity of 316 L stainless steel can be applied surface alteration such as passivation, anodization, and nitrogen implantation (Bordjih et al., 1996).

2.2.2 Cobalt Alloys

In 1940s the CoCrMo alloy which called as Vitalliums were utilized as a orthodontic alloy and than complied with orthopedic operations (Chen & Thouas, 2014).

Essentially cobalt chromium alloys divided two categories: First the castable Co-Cr-Mo alloys and secondly the wrought forging Co-Ni-Cr-Mo alloys which called as MP35N (Standart Presses Steel Co.). Metallic castable CoCrMo alloy has been utilize for many years in medical operations. The wrought forging Co-Ni-Cr-Mo alloys are comparatively new, now utilized for prostheses for joints for instance knee and hip. CoNiCrMo (MP35N) contains 35% Co and Ni. The alloy has good corrosion resistant to salty solution (e.g. seawater) under stress. CoNiCrMo alloy is proper for medical

operations which require stress fatigue and long operation life without crack forming (Aherwar, Singh, & Patnaik, 2016).

2.2.3 Titanium and Titanium Alloys

Titanium and Titanium alloys was founded by William Gregor in England at 1791 and named by Martin Heinrich Klaproth for the Titans of Greek mythology (Levitus & Boyer, 1994). The use of titanium for biomedical products manufacturing dates to the 1930s. It was discovered that titanium could be tolerated in bone, as was Vitallium (CoCrMo alloy) and stainless steel (Niinomi, 2019).

Titanium is one of the transition elements in group IV and period 4 of periodic table. Titaniums have an inadequately filled d shell in its atomic system. Supplies of pure titanium are rare, though titanium ores such as ilmenite and rutile are very common. Titanium alloy has well tensile strengt, toughness, low density, excellent corrosion behavior. However, high cost of resources, their usage limits to military applications, aircraft, medical tools and consumer electronics. Allotropic transformation of Titanium at 885 °C, and change from a hexagonal closest packed (α phase) to body centered cubic crystal (β phase) (Mouritz, 2012).

Titanium metallic alloys are seperated into four groups: These are, α alloys, α-β alloys, and β alloys. Table 2.4 lists ASTM and UN standards for titanium and its alloys utilized for biomedical applications (International, 2003).

Table 2.4 UN/ASTM standards for titanium and its alloys

Category	ASTM	UN Standard No	Materials
α microstructure	F67	R50250	Commercially pure Ti grade 1
		R50400	Commercially pure Ti grade 2
		R50550	Commercially pure Ti grade 3
		R50700	Commercially pure Ti grade 4
α-β microstructure	F136	R56401	Ti6Al4V ELI
	F1472	R56400	Ti6Al4V
	F1295	R56700	Ti6Al7Nb
	F2146	R56320	Ti3Al2.5V
β microstructure	F1713		Ti13Nb13Zr
	F1813	R58120	Ti12Mo6Zr2Fe
	F2066	R58150	Ti15Mo

Ti6Al4V and its low Interstitial variant Ti6Al4V ELI and Commercially pure titanium (CP-Ti) grades are most broadly utilized in biomedical applications. The addition of alloying element to titanium enables it to has a broad range of features. For example, Aluminum is inclined to stabilize the α phase and improve the transformation temperature from α to β phase. Vanadium tends to stabilize the β phase by lowering temperature of the transformation α to β phase (Zhou et al., 2019).

Commercially pure titanium (unalloyed titanium CP Ti) is categorized into four class (Table 2.5) and firstly based on its content of O (oxygen) and Fe (iron) (Muñoz & Costa, 2012).

Table 2.5 Impurity limits of commercially pure titanium (CP-Ti)

Materials	Nitrogen	Carbon	Hydrogen	Fe	Oxygen
ASTM grade 1	0.03	0.08	0.015	0.2	0.18
ASTM grade 2	0.03	0.08	0.015	0.3	0.25
ASTM grade 3	0.05	0.08	0.015	0.3	0.35
ASTM grade 4	0.05	0.08	0.015	0.5	0.40

Titanium and its alloys are light weight and have good mechanic and chemical features are significant properties for medical application. Physical and mechanical properties of implant metals and their alloys used in medical applications shown at Table 2.6 (Blau, 1992).

One of Titanium alloy,which written as Ti6Al4V is one of the frequently utilized biomaterials in medical operations for instance artificial hip and patella joint due to its biocompatibility, perfect corrosion performance and mechanical features. Nonetheless, its good known fundamental challenge of bad wear performance has finited the commonly utilize of biomedical Ti6Al4V. Furthermore, in the body, circumstantial action of wear and corrosion may occur to increased deteriortaion of the biomaterials and create high wear detritus, which will limit the long term steady of load bearing biomaterials. Accordingly, it is required to increase the wear resistance of Ti6Al4V in aggresive body fluids and enhanced the operation life by surface alteration methods. Many investigations have been searched on increasement of wear performance of Ti6Al4V by surface treatment, micro arc oxidation and thermal oxidation (Zhou et al., 2019).

Table 2.6 Physical and mechanical features of metallic biomaterials (Blau, 1992)

		316L	CoCrMo alloy	cp Ti	Ti6Al4V
Density (g/cm^3)		7.90	7.80	4.50	4.40
Young's modulus (GPa)		200	200	127	111
Tensile Strength (MPa)		465	665	575	900
0.2% proof stress (MPa)		170	455	465	830
Fracture strain, %		40	10	15	8
Fatigure stress (MPa)	Air	241	290	250	380
	Saline	103	140	120	140

2.3 Ceramic Biomaterials

Ceramics are polycrystalline compounds with interatomic bonding as ionic or covalent, generally anorganic and including silicate, oxide, carbide, and different sulfide and selenide (Pierson, 1996).

Ceramics are attractive as implants due to the biocompatible features for instance bioinert, biodegradable and bioactive. The most frequently used ceramic implant materials include aluminum oxides (Al_2O_3), calcium phosphates (CaP), zirconium oxides (Zr_2O_3), magnesium oxides (MgO), apatites, graphites and glasses. Bioceramics are used as medical applications to repair parts of human body, usually the skeletal system, for instance bones, teeth or joints.

Recently, use of bioceramics were limited due to their brittleness, susceptibility to microcracks, bad tensile and bad impact performance. For this reason their achivement related with their ability to persuade bone reclamation and bone in spread at the tissue-implant interface. In order to classify of a ceramic biomaterial, the ceramic materials must exceed such features:

- nontoxic
- noncarcinogenic
- nonallergic

- noninflammatory
- biocompatible
- should be bio-functional for its lifetime in the host (Baino, Novajra, & Vitale-Brovarone, 2015).

Table 2.7 shows biomedical applications of bioceramics (Thamaraiselvi & Rajeswari, 2004). These applications and repairs become necessary when the existing part becomes diseased, damaged, or just simply wears out.

Table 2.7 Biomedical applications of bioceramics

Implants	**Function**	**Bioceramic materials**
Artificial total hip, knee, shoulder, elbow, wrist	Reconstruct arthritic or fractured joints	High-density alumina, metal bioglass coatings
Bone plates, screws, wires	Repair fractures	Bioglass-metal fiber composite,
Intramedullary nails	Align fractures	Bioglass metal fiber composite, Polysulfone-carbon fiber composite
Harrington rods	Correct chronic spinal curvature	Bioglass-metal fiber composite, Polysulfone-carbon fiber composite
Permanently implanted artificial limbs	Replace missing extremities	Bioglass metal fiber composite, Polysulfone-carbon fiber composite
Vertebrae Spacers and extensors	Correct congenital deformity	Al_2O_3
Spinal fusion	Immobilize vertebrae to protect spinal cord	Bioglass
Alveolar bone replacements, mandibular reconstruction	Fixing the alveolar ridge to improve denture fit	Polytetra fluro ethylene - carbon composite, Porous Al_2O_3, Bioglass, apatite
End osseous tooth replacement implants	Replace diseased, damaged or loosened teeth	Al_2O_3, Bioglass, dense hydroxyapatite, vitreous carbon
Orthodontic anchors	Provide posts for stress operation required to change deformations	Bioglass-coated Al_2O_3, Bioglass coated vitallium

2.3.1 Alumina (Al_2O_3)

Since 1975 alumina ceramic has proven its bioinertness. Alumina ceramics has characteristics of high hardness and high tribological performance. Natural alumina is known asruby (Thamaraiselvi & Rajeswari, 2004).

The single crystal structure of Al_2O_3 has been used to produce implants for biomedical applications. The alpha alumina (α-Al_2O_3) has a hexagonal close packed ctystal form. The origin of purity Al_2O_3 is bauxite and corundum. The chemical composition and density of pure calcined Al_2O_3 is shown at Table 2.8 (Wiederhorn & Bolz, 1970).

Table 2.8 Chemical content of calcined alumina (Wiederhorn & Bolz, 1970)

Chemical Content	Amount (weight %)
Al_2O_3	99.6
SiO_2	0.12
Fe_2O_3	0.03
Na_2O	0.04

The Alumina's strength related with particle size. Physical equity conditions of Al_2O_3 biomaterials given at Table 2.9 (Testing & Materials, 2000).

Table 2.9 ASTM standards of physical conditions of alumina implants

Features	Values
Flexural strength	>400 MPa (58.000 psi)
Elastical modulus	380 GPa (55.1 x 10^6 psi)
Density	3.8-3.9

The biocompatibility of Al_2O_3 has been performed by many investigators. The reaserches reported that, there is no evidence about implant rejection of the implanted sample (Zavan, 2017).

2.3.2 Zirconia (ZrO_2)

Zirconium Oxides or with other name is Zirconia (ZrO_2) have been tried for operation in biomedical applications. The advantages of ZrO_2 in load bearing implant are its lower modulus of elasticity and higher strength. The mechanical features are better than Al_2O_3. ZrO_2 is very biocompatible as other bioceramics and can be produce large size implants for instance the acetabular implant in hip joint application (Bronzino, Wong, & Peterson, 2012).

The high resistance of partially stabilized zirconia (i.e. Y-TZP means Yttria-stabilized tetragonal zirconia polycrystal) against crack propagation is based on a phase transformation from tetragonal to the monoclinic phase. This transformation leads to a volume expansion of 3% to 4%. The energy associated with fracture multiplication is depleted in the phase changing and in over-coming the compression stresses caused by volume growth (Wenz, Bartsch, Wolfart, & Kern, 2008).

2.3.3 Calcium Phosphate ceramics

The Calcium phosphate belong to the orthophosphate class and naturally occur in some biological complexes, including bone. Bone formed from an anorganic composition of biological apatites (CaP) and an organic content, consisting primarily of collagen (Samavedi et al., 2013).

Latterly, this chemicals have been produced and utilized for producing different forms of biomaterials as well as for solid coatings on other biomaterials. There are mono calcium phosphates, di calcium phosphates , tri calcium phosphates , and tetra calcium phosphates, also the HAP and β whitlockite, which has ratio of 5/3 and 3/2 for calcium and phosphorus (Ca/P). The steadily in suspension commonly extends with extending Ca/P ratio (Park & Lakes, 2007).

The bone minerals are compose of non stoichiometric and polysubstituted Calcium phosphate, CaP was quickly choosed as they can be part of the bone redesign process.

Based on its formation, CaP presently used as implants are seperated as calcium $Ca_{10}(PO_4)_6(OH)_2$ alpha tricalcium phosphate (α - TCP) or beta tricalcium phosphate (β - TCP) , $Ca_3(PO_4)_2$; biphasic calcium phosphates (BCPs) for mixtures of HAP and β-TCP; and non-sintered apatites or lack of calcium apatites which named as calcium-deficient apatites (CDA). HAP and β - TCP can be prepared by grounding CaO and P_2O_5 particles with Ca/P equals to 1.67 and 1.5 in Table 2.10 (Samavedi, Whittington, & Goldstein, 2013).

Table 2.10 Summary of key CPC features that influence osteoblastic differentiation (Samavedi et al., 2013)

Name (CPC)	**Values of Solubility (K_{sp})**	**Ratio of Ca/P**	**Performance of Osteoinductivity**
HAP	Low (10^{-58})	1.67	•
TCP	Normal (10^{-25}–10^{-29})	1.5	••
ACP	High (10^{-23}–10^{-25})	from 1.15 to1.67	•••
BCP	Variable (depend on TCP/HAP)	from 1.5 to1.67	••••

Table 2.11 shows the major names of the CaP group that are interest to implant operations, consistent with their Ca/P ratios, their pH stability range in suspensions.

Table 2.11 The calcium phosphate family and their names with formula for coatings in orthopaedic devices (Jansen & Leon, 2009; Shadanbaz & Dias, 2012)

Ca/P Molar Ratio	Name of CPC	Chemical Formula	pH Stability Value
0.5	MCPM (monobasic calcium phosphate monohydrate)	$Ca(H_2PO_4)_2 \cdot H_2O$	0.0-2.0
1.0	DCPA (dicalcium phosphate anhydrous, Monetite)	$CaHPO_4$	2.0–5.5 (>80 °C)
1.0	DCPD (dibasic calcium phosphate dehydrate, Brushite)	$CaHPO_4 2H_2O$	2.0–6.0
1.33	OCP (octacalcium phosphate)	$Ca_8(HPO_4)_2(PO_4)_4 5H_2O$	5.5–7.0
1.5	α-TCP (α-tricalcium phosphate)	$\alpha\text{-}Ca_3(PO_4)_2$	Precipitated from suspensions
1.5	β-TCP (β-ticalcium phosphate)	$\beta\text{-}Ca_3(PO_4)_2$	Precipitated from suspensions
1.5	ACP (amorphous calcium phosphate)	$Ca_xH_y(PO_4)_z nH2O$, n = 3–4.5, 15%-20% H2O	~5–12 1
1.2-2.2	CDHA (calcium deficient hydroxyapatite, CDHAp; precipitated HAp, pHA, pHAp)	$Ca_{10-x}(HPO4)_x(PO_4)_{6-x}(OH)_{2-x}$ $(0 < x < 2)$ [2]	6.5–9.5
1.5-1.67	HAp, or OHAp (Hydroxyapatite)	$Ca_{10}(PO_4)_6(OH)_2$	9.5–12.0
2.0	TTCP	$Ca_4(PO_4)_2O$	Precipitated from suspensions

Stoichiometric Hydroxyapatite (HAP) has the chemical formula $Ca_5(PO_4)_3(OH)$. However, it is commonly named as $Ca_{10}(PO_4)_6(OH)_2$ (Table 2.11 to indicate that the hexagonal cell is comprised of two molecules (Dorozhkin & Epple, 2002). International Union of Pure and Applied Chemistry (IUPAC) classification, it is pentacalcium hydroxide tris (phosphate) (Dorozhkin, 2012). Hydroxapatite is the second stable and soluble after fluorapatite (FAp) of all Calcium phosphates. HAP contributes nucleating sites for precipitation of apatite in medium and in blood (Samavedi et al., 2013). Hydroxyapatite is bioactive but also osteoconductive, non

toxic, non immunogenic, and its formation is crystallographically similar to bone (Murugan & Ramakrishna, 2005). The term Tricalcium phosphate is utilized in its rigorous chemical meaning to nominate phases written as $Ca_3(PO_4)_2$ with a Ca/P ratio is 1.5. Crystalline Tricalcium phosphate (α - and β - TCP) is synthesised only with sintering process; it is commonly obtained that crystalline TCP cannot be produced directly solution (Heughebaert, Zawacki, & Nancollas, 1983). α-TCP is generally made from β-TCP by sintering at 1125 °C and prevent the reverse conversion. Although α-TCP and β-TCP have the same chemical content, their solubility and crystal structure are shown difference (Yin, Stott, & Rubio, 2003).

β-TCP has rhombohedral space family, and its unit cell comprises twenty one $Ca_3(PO_4)_2$ formula units. There are three types of crystallographic nonequivalent PO3 and PO4 groups located at common points of the crystal, each type with various intra tetrahedral bond lengths and angles (Kamminga et al., 2019). Both HAP and β-TCP have similar FTIR spectrum, (Wang & Nancollas, 2008).

2.3.4 Bioactive Glass Ceramics

Glasses are polycrystalline ceramics produced by crystallization of glasses. They were originally established by Corning Glass Works in the 1960s. Firstly used in photosensitive glass ceramics which contains copper, silver and gold are coated by UV light. These metallic coatings force to nucleate and crystallize the glass into a slim grained glass which possess perfect mechanical and thermal features created for biomedical applications (Park & Lakes, 2007).

Unfortunately bad properties of the glasses are their brittleness. Additionally, restrictions on the contents utilized for manufacturing biocompatible glass hinders the fabrication of a glass which has substantially better mechanical performance. So, glasses cannot be used for making load bearing medical implants. Nevertheless, glasses may be utilized for bone cement, orthodental fixing composites, and coating biomaterial (Park & Kim, 2003).

CHAPTER THREE
PRODUCTION OF CaP COATINGS

Many methods to obtain Calcium Phosphate coatings on metallic substrates. There are different methods have been engaged to achieve CaP based most often HAP coatings with attractive properties including particle as well as solution techniques such as liquid plasma spraying (PS), radio-frequency (RF) magnetron sputtering, direct current (DC) magnetron sputtering, electrophoretic deposition (EPD) pulsed laser deposition (PLD) or consolidation of disparate methods (Wang & Nancollas, 2008).

3.1 Plasma Spraying

Plasm spraying technique is commonly utilized technique for deposit Hydroxyapatite coating on biomaterials (Liu et al., 2017). These approaches is very high used for orthodental and orthopaedic biomaterials. The indirect technique of plasma spray uses melting and spraying onto the substrate by a method an plasma via electric arc. The process involves heating the particle via plasma. Plasma spraying can be applied under vacuum, controlled environments. (Harun, Asri, Sulong, Ghani, & Ghazalli, 2018).

The temperature at the center region of plasma exceeds about 29.726 °C. The ions and electrons in plasma is divorced and they are speed up to the electrodes (cathode and anode). Figure 3.1 shows schematic illustration of plasma spray coating method. These moving powders then clash with other molecules in the transfering gas, which results in enlargement owing to the heat escalation. After, a plasma is created that throws off from the nozzle toward the implant surface at momentums approaching the mach speed which is speed of sound. Then, ceramic powders are gived into the plasma. The powders melt and are coated on the implant surface at which the nozzle is targeted. The quality of plasma spray depositions can be effected by some parameters, for instance the temperature of flame, the plasma gas, powder size, and the chemical composition of the ceramic particle (Jansen & Leon, 2009). Typically used plasma

gasses are Helium, Argon, Nitrogen, Hydrogen and mixing of these gasses. Generally preferred gas is the Argon and used as the main gas as it ionizes efficiently and contributes a balanced arc under electrical field (Brunette, Tengvall, Textor, & Thomsen, 2012).

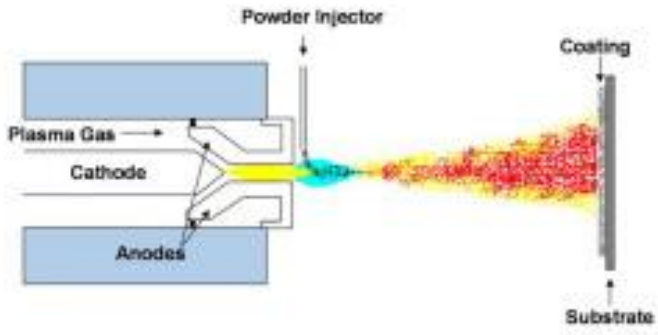

Figure 3.1 Schematic of Plasma Spray technique (Levingstone, Ardhaoui, Benyounis, Looney, & Stokes, 2015)

Plasma spraying technique has many problems such as; decomposition of Hydroxyapatite,formation ofamorphous calcium phosphate (ACP), and fracturing. Plasma sprayed HAP coating commonly contains tricalcium phosphates (TCP in α or β structure), oxyhydroxyapatite (OHA), tetracalcium phosphate (TTCP), and calcium oxide (CaO) with various features (Roy, Bandyopadhyay, & Bose, 2011).

3.2 Magnetron Sputtering

Magnetron sputtering technique to form calcium phosphate deposition on metallic implants were known at the 20th century (Pichugin et al., 2008).

Radio frequency magnetron sputtering technique one of the most auspicious and generally utilized technique for obtain bioactive coatings on medical biomaterial substrates (Fedotkin et al., 2019).

Radio frequency (RF) sputtering in an electric field is a accepted method used to coat an implant surface. Figure 3.2 shows schematic illustration of magnetron sputtering coating method. The principles of the method involve depositing an aimed

material onto am implant surface by bombarding the aim via ionized Argon atoms (Helmersson, Lattemann, Bohlmark, Ehiasarian, & Gudmundsson, 2006).

RF Sputtering technique is a works in a vacuum environment via bombardment with high-energy ions. The common design for the formation of Calcium phosphate includes vacuum chamber, RF generator, magnetron, and chiller system for cooling the setup (Surmenev, 2012).

Therefore, RF magnetron sputtering technique makes a critical impact in application fields including hard, wear performance, low friction, corrosion resistant, specific optical films, electrical features (Kelly & Arnell, 2000).

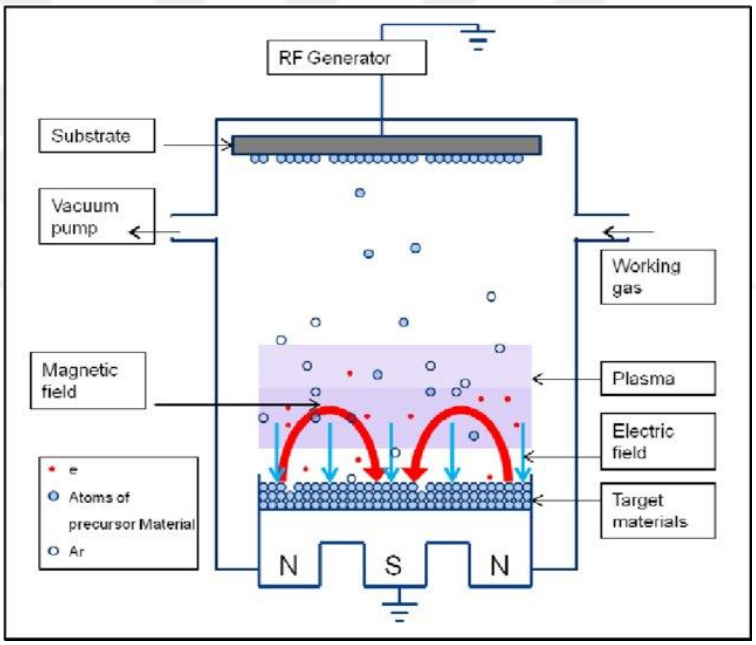

Figure 3.2 Schematic of Magnetron Sputtering (Bosco, Van Den Beucken, Leeuwenburgh, & Jansen, 2012)

3.3 Sol-gel Derived Coatings

The technique of Sol–gel has been good developed to form different materials because the methods have some advantages , for instance, easy control of chemical reactions and synthesis at low temperature these are critical for film creation via sol-gel method (Weng et al., 2003). Figure 3.3 shows Sol-gel technique.

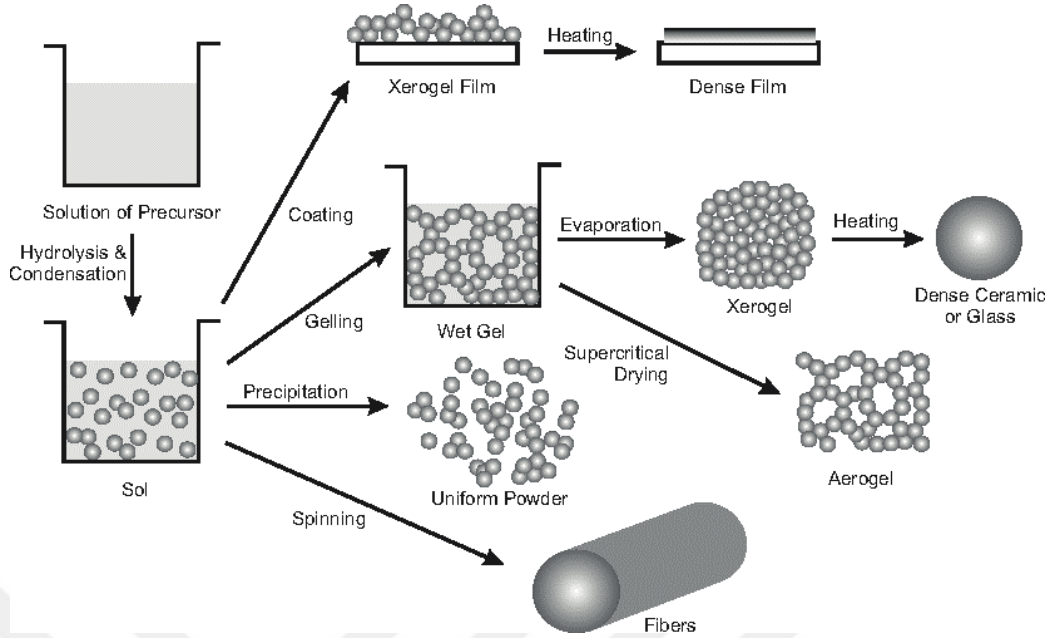

Figure 3.3 Sol–gel technique process (Nyamukamba, Okoh, Mungondori, Taziwa, & Zinya, 2018)

Sol–gel method is attractive to deposit Hydroxyapatite coatings due to excellent features for instance, low temperature, the possibility totailor structure and morphology and easiness for complicated shaped specimens (Azem, Eroglu, & Cakir, 2011).

3.4 Electrodeposition

Electrochemical coating technique of metallic materials and affects the contraction of metallic ions from solution, organic, and salty solutions. The decreasing of metallic ions M^{z+} in solution is represented by;

$$M^{z+}_{solution} + ze \longrightarrow M_{lattice} \tag{3.1}$$

This can be consummated by means of two various steps: (1) electrodeposition process in which *z* electrons (e) are arranged by external power, and (2) electroless coating process which a decreasing agent in the suspension is the source of electron . These two steps, electrodeposition and electroless coating, creating electrochemical coating (Paunovic & Schlesinger, 2006).

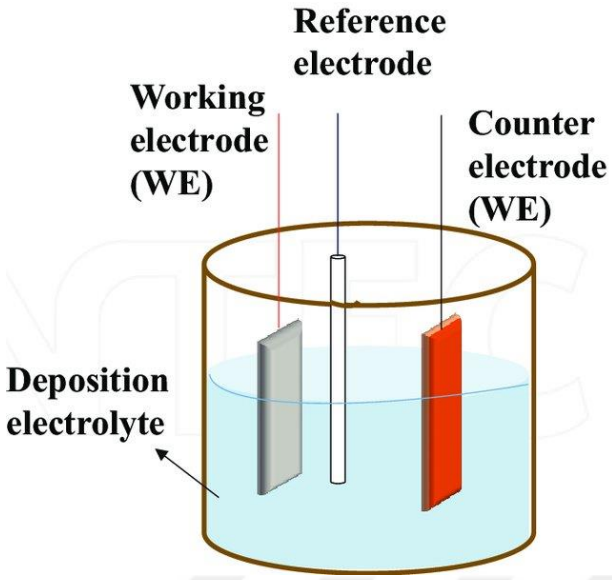

Figure 3.4 General electrodeposition setup (Yi & Majid, 2018)

Electrochemical techniques are progressively used for the deposition coatings. Different cathodic reactions of electrochemical techniqe, the following chemical reactions which deplete Hydrogen and generate OH^- include the contraction of water, dissolves oxygen, nitrate and chlorate ions (Zhitomirsky, 2002).

$$2H_2O + 2e^- \rightarrow H_2 + 2OH^- \quad (3.2)$$

$$NO_3^- + H_2O + 2e^- \rightarrow NO_2^- + 2OH^- \quad (3.3)$$

$$O_2 + 2H_2O + 4e^- \rightarrow 4OH^- \quad (3.4)$$

$$NO_3^- + 7H_2O + 8e^- \rightarrow NH_4 + 10OH^- \quad (3.5)$$

$$ClO_4^- + H_2O + 2e^- \rightarrow ClO_3^- + 2OH^- \quad (3.6)$$

$$ClO_4^- + 4H_2O + 8e^- \rightarrow Cl^- + 8OH^- \quad (3.7)$$

The disadvantage of the electrodeposition technique; For extra electrochemical circumstances (high current density, long span polarization) there is a hydrogen embrittlement risk for metallic biomaterials (Rößler et al., 2003).

3.5 Electrophoretic Deposition

Electrophoretic deposition technique (EPD) is a colloidal method in which charged powders in a suspension motion and deposit on an oppositely charged electrode for make coatings via electrical field (Ma, Han, Wang, Chen, & Jia, 2018).

Spesific coatings, for instance superconductive, magnetic, and biocompatible coatings can be made by EPD (Besra & Liu, 2007). Solid powders can be easily coated via EPD method (particle size should be <30 micron) . The advantages of the EPD technique are; easy setup, forming the coating at room temperature, low cost, not long deposition period, ability to homogeneous depositions with controlled thickness on complex designed implant surfaces, possibility of co-deposition of various powders, and comparatively high adhesion strength (Augello & Liu, 2015). Furthermore, EPD setup may be upgraded to bigger product. The conductive surfaces of components can be deposited with EPD; the method also give permisson to infiltrate non conductive sample surfaces. The critical difficulty of EPD are the requirement of forming steady solutions, and the electrochemical reactions (Amrollahi, Krasinski, Vaidyanathan, Tayebi, & Vashaee, 2016). A typical EPD setup has a power souce, anode, cathode and a steady solution as shown in Figure 3.5. EPD has two process: electrophoresis step and, deposition step (Amrollahi et al., 2016).

The electrophoresis process, charged and dispersed powders in a solvent progress toward the working electrode. In the second process, powders coagulate on the electrode, and homogeneous coating is formed. The positively charged powders forms on the negative electrode which called as cathode whereas negatively charged powders deposit on the anode (Chhetri, Kuila, & Murmu, 2016). These two process steps are referred as cathodic deposition and anodic deposition method, respectively (Paunovic, 2007).(Aliofkhazraei et al., 2016).

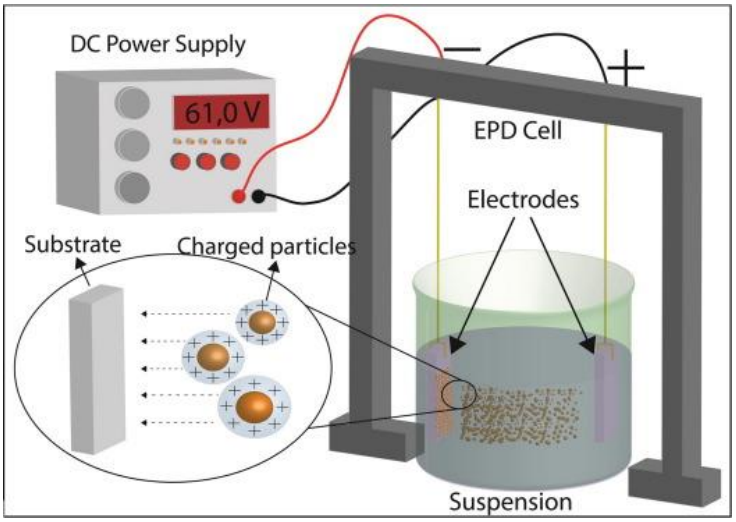

Figure 3.5 Schematic of an Electrophoretic cell (Amrollahi et al., 2016)

Many works have been documented to explain the particle interaction and kinetics of electrophoretic coating. There are various coating methods available for CaP coatings. EPD gained more attention due to the properties of good stoichimotery control, high purity of the deposited material and rapid processing (Boccaccini, Keim, Ma, Li, & Zhitomirsky, 2010). Many studies have been investigated for Calcium phosphate coatings on different metallic materials with EPD method. The metallic substrates such as Titanium and Titanium alloys (Ti6Al4V) (Wei et al., 1999), meshes (Ducheyne, Radin, Heughebaert, & Heughebaert, 1990), stainless steel (Guo, Fang, Wang, Yang, & Xu, 2011), aluminium, brass (Esfehanian, Raissi-Dehkordi, & Moztarzadeh, 2005) and carbon fibres (Zhitomirsky, 1998) have been considered for electrophoretic deposition of Calcium phosphate. The EPD of CaP depends on electrokinetic properties, which is influenced by pH of the solution, concentration of particles, distribution of particle size, shape and surface area of the particles (Kowalchuk, Pollack, Ducheyne, & King, 1993). The citric acid was used as a dispersant and it permits the deposition from aqueous and non-aqueous solvents. The deposited biomaterials were then used for hip prosthesis applications. The HAP coating adherence and strength was improved by addition of PVA in the EPD suspension (Meng, Kwon, Yang, Ong, & Kim, 2006). However, careful selection of dispersants is essential because,in biomedical applications some of the additives cause toxic or adverse to the cells. Many studies have been carried out to research the influence of the applied electric field on the deposition rate and morphology

of the obtained Hydroxyapatite. The high voltage offers faster deposition rate and yields higher deposition thickness within short duration of time (Zhitomirsky & Gal-Or, 1997). But then, high electrical field or high voltage creates agglomeration of fine powders in the process and it was found that, the particles size become larger and the porosity of the coating was increased (Meng et al., 2006).

3.5.1 Processing parameters

The critical factors, influencing Electrophoretic deposition has been researched by Besra and Liu (Figure 3.6), and include voltage, coating time and suspension properties.

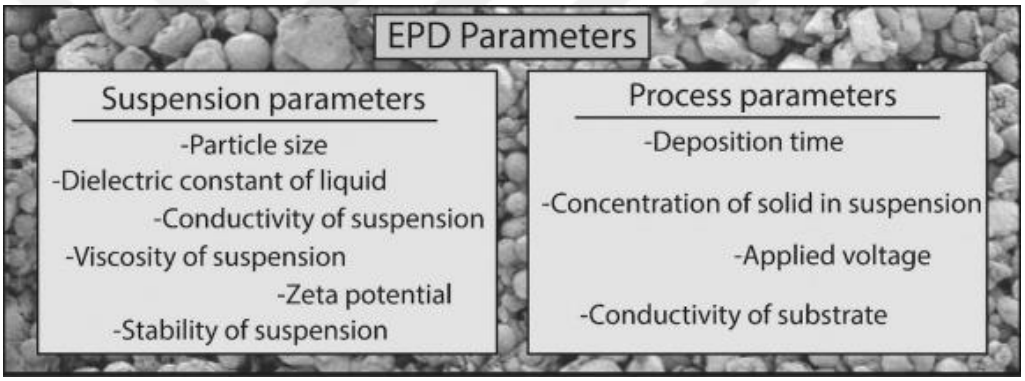

Figure 3.6 Key EPD processing parameters (Avcu et al., 2019)

The physical features of powders and suspension must be controlled sensitively. Particle surface chemistry, surface and liquid interfaces behavior under voltage and the forming powder-powder and powder-sample surface networks define the quality of EPD (Filiâtre, Pignolet, & Buron, 2017). A steady solution having good dispersed and controlled substrate charged powders is crucial for EPD. Steady suspensions show no tendency to flocculate which maintains the creation of denser and stronger adhered coatings while flocculating soltions settle speedly and causes the creation of a washily adhered coating with low density (Larsson, Hill, & Duffy, 2012).

The most critical mechanisms for the steadiness of EPD solutions are the ionisation of surface groups on powders (electrostatic steadiness) and the adsorption of

surfactants (electrosteric stabilisation) (Besra & Liu, 2007). Figure 3.7 shows the schematic of electrostatic and steric stabilisation.

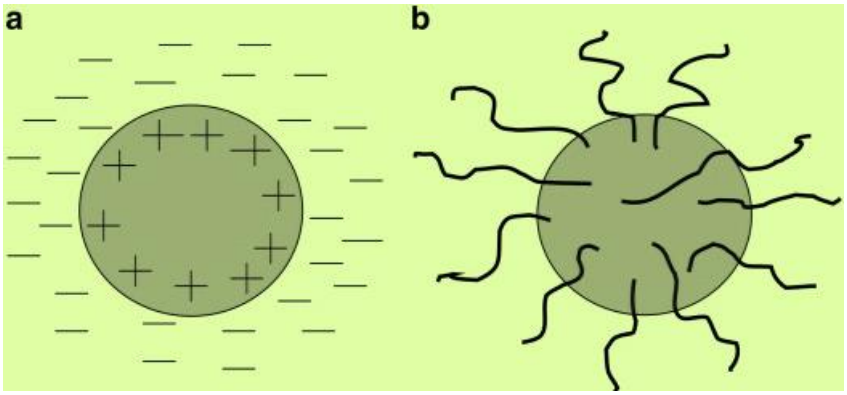

Figure 3.7 Schematic draw of stabilisations model (a) electrostatic and (b) steric (Besra & Liu, 2007)

Depending on pH, electrolyte density, the particles in the area close to the deposit coating reciprocavitely repulse (steady state), weakly attract (flocculated state) or strongly attract (coagulated state) (Besra & Liu, 2007).

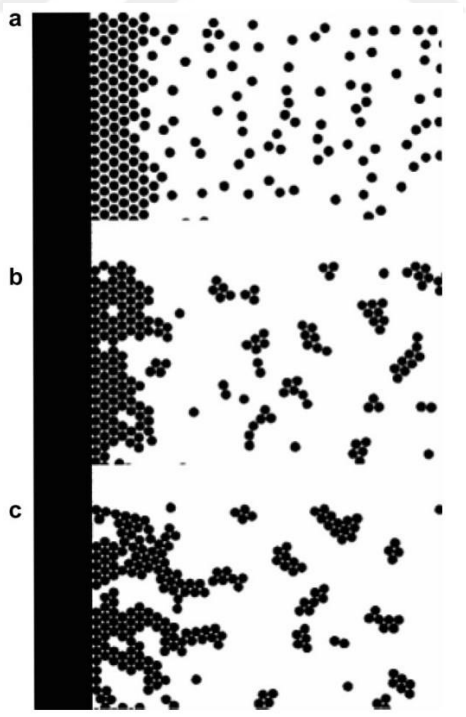

Figure 3.8 Schematic of particle distribution (a) stable state; maximum packing density, (b) flocculated state; particles are weakly bound, (c) agglomerated state (coagulated state); non-uniform packing structure (Cordelair & Greil, 2004)

In the steady status the powders form a highly ordered deposit with a deposition density on the electrode, Figure 3.8 (a). Creation of areas the powders are weakly bind to each other characterizes the flocculated status, Figure 3.8 (b). These aggregates accumulate at the electrode forming a non-uniform packing structure where domains of high order are interconnected Figure 3.8 (c) (Cordelair & Greil, 2004).

After the deposits via EPD technique, sintering process is generally needed to forming strong and denser coating. High temperature applications shows some problems, for instance the shrinking of coatings, the difference between thermal expansion performance of the sample and the depositions on substrate leading to fracture of films, the potential unwanted reactions between the implants and the deposited films, structural decomposition of samples with increased temperature. However, a sintering process is not generally desired for polymers deposits (Avcu et al., 2019).

CHAPTER FOUR
EXPERIMENTAL STUDIES

4.1 Preperation of the Electrolyte

Suspensions of electrophoretic deposition process were prepared by adding commercial HAP powder (Sigma-Aldrich, CAS: 1306-06-5) to n-butanol (Merck, CAS: 71-36-3) with different amounts of diethanolamine (DEA) (Sigma-Aldrich CAS: 111-42-2) . Table 4.1 summarizes the ingredients of prepared suspensions. The suspension were dispersed for 30 minutes with magnetic stirrer and 30 min with ultrasonically bath before deposition process.

Table 4.1 Ingredients of prepared suspensions

Abbreviation	Stirring Time (min.)	Ultrasonic Time (min)	Dispersant (g/L)	HAP (g/L)	Alcohol (ml)
S1	30	30	0	40	500
S2	30	30	2	40	500
S3	30	30	6	40	500
S4	30	30	10	40	500

4.2 Characterization of Electrolyte

Four different characterization techniques were used for characterizaiton of electrolytes. These are pH, electrical conductivity, average particle size and zeta potential measurements.

4.2.1 pH and Conductivity Measurement

The electrical conductivity and pH values are important parameters of suspensions. These parameters play an important role for stability of suspensions. For instance the increment of the pH causes a great amount of positive ion to increase which effect the zeta potential. The electric conductivity and pH measurements of the suspension was determined by a Mettler Toledo S47-K SevenMulti dual meter pH/conductivity meter.

4.2.2 Zeta Sizer and Particle Size measurement

Zeta potential is a parameter characterizing electrochemical equilibrium on interfaces. It depends on the properties of liquid as well as on properties of the surface. It plays an important role in theory of aggregative stability. The electrical state of a charged surface is determined by the spatial distribution of ions around it. Such a distribution of charges has traditionally been called EDL, although it is often more complex than just two layers, and some authors have proposed the term "electrical interfacial layer". Zetasizer Nano-ZS Malvern was used to measure the particle size of commercial HAP powder and zeta potential of prepared suspensions (Larsson, Hill, & Duffy, 2012).

4.3 Preperation of the Substrates

Ti6Al4V alloy with the dimensions of 100 mm x 25 mm x 1.5 mm were used as the substrate. The plates of Ti6Al4V alloy were abraded with 600-grit silicon carbide paper. After abrading, substrates were etched with a solution containing 15% nitric acid (HNO_3), 5% hydrofluoric acid (HF) followed by washing with acetone in an ultrasonic bath for 10 min, then washing with distilled water and then dried at room temperature .

4.4 Deposition of Coatings

Deposition of coatings on prepared substrates were performed with an electrophoretic cell using pure titanium and Ti6Al4V alloy plates as cathode and 316L plate as anode which were connected to an electrophoresis apparatus. The distance between cathode and anode was 1 cm. schematic illustration of an EPD system is shown in Figure 3.5. The deposition process was conducted at three different voltage values of 40 V, 50V and 60 V for 45 minutes at room temperature. Abbreviation of the deposited coatings were shown at Table 4.2.

Table 4.2 Abbreviation of the produced coatings

Abbreviation	Substrate Properties (Ti6Al4V)	Coating Time (min)	Dispersant (g/L)	HAP (g/L)	Alcohol (ml)	Voltage (V)	Sintering (°C)
E60-D0	Etched	45	0	40	500	60	800
E60-D2	Etched	45	2	40	500	60	800
E60-D6	Etched	45	6	40	500	60	800
E60-D10	Etched	45	10	40	500	60	800
E50-D0	Etched	45	0	40	500	50	800
E50-D2	Etched	45	2	40	500	50	800
E50-D6	Etched	45	6	40	500	50	800
E50-D10	Etched	45	10	40	500	50	800
E40-D0	Etched	45	0	40	500	40	800
E40-D2	Etched	45	2	40	500	40	800
E40-D6	Etched	45	6	40	500	40	800
E40-D10	Etched	45	10	40	500	40	800

After EPD process, coated specimens were dried at room temperature and then sintered in tubular furnace at 800 °C for 2 h with argon gas with a heating rate of 1 °C/min until 200 °C and 5 °C/min from 200 °C to 800 °C. Finally cooling rate to room temperature was 1 °C/min.heat treatment profile of deposited coatings are given in Figure 4.1.

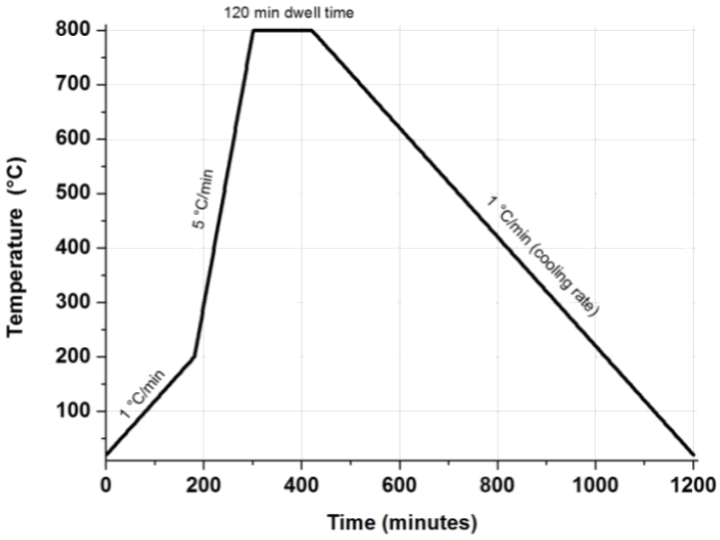

Figure 4.1 Heat treatment profile of coatings

4.5 Characterization of deposited Coatings

4.5.1 X-Ray Diffractions (XRD)

XRD is a common method for identify the crystalline phases for materials and measure the structural features phases. XRD is not contact and non destructive. The ordinary array of atoms in a crystalline material creates a 3D diffraction grating for waves with a wavelength around that of the distance between the atoms. When waves attempt to crystal, they are scattered in all directions by the atoms. In certain directions, these waves can interfere destructively. In other directions, constructive interference will appear resulting in spectrum peak in X-ray intensity (Ahmed, Jackson, & Jackson, 2009). The diffraction spectrum lattice of the crystal can be used to define the crystal structure. Bragg's law is the main formula for define diffraction of crystal:

$$n.\lambda = 2.d.\sin\theta \qquad (4.1)$$

n is an integer known as the order of diffraction, λ is the X-ray wavelength is the gap between two sequentially dividing planes and θ is the angle between the atomic planes and the incident X-ray (Ahmed, Jackson, & Jackson, 2009). Figure 4.2 illustrates diffraction of x-rays by planes consist of atoms.

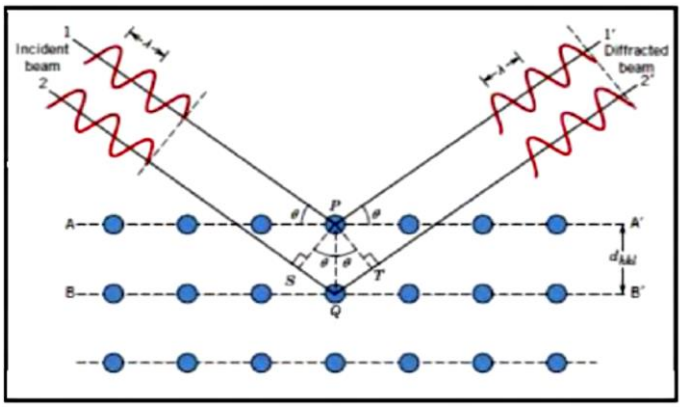

Figure 4.2 X -ray diffraction by planes of atoms (A -A ' and B -B ') (Callister Jr & Rethwisch, 2012)

In this study, X-ray diffraction (XRD) datas were collected via XRD diffractometer with Cu K_α radiation (Thermo-Scientific, ARL-K_α) over the 2θ range from 20° to 90° at 0.02°/s (2θ) was applied to define the phase of deposited coatings.

4.5.2 Scanning Electron Microscopy (SEM)

Scanning electron microscopy (SEM) is the most common analytical techniques to analyse surface morphology of the solid-state samples. The electron beam created by an electron source, elevated by high voltage, and focused on the specimen by a series of electromagnetic lenses scans the the specimen by means of a series of deflection coils and synchronized with a cathode ray tube (CRT). The signals created as a result of the beam interaction with the sample is assembled by a suitable receiver, amplified, and displayed on the monitor (Michael, 2011).

The energy dispersive spectroscopy (EDS) is often attached to the SEM. The X-rays generated from the interaction between the electron and the specimen is used to identify and measure quantitatively the elemental composition of the sample. Therefore, SEM/EDS can specify the elemental composition and obtain the morphology of the sample simultaneously.

In this study, the surface morphology and elemental analyse of the coatings were determined by using JEOL-JSM 6060 Scanning Electron Microscopy with an Energy Dispersive X-ray spectroscopy system attachment.

4.5.3 Fourier Transform Infrared Spectroscopy (FTIR)

Fourier Transform Infrared (FTIR) spectroscopy is generally a non destructive method, which is used to determine the absorption of different infrared light wavelengths of organic or inorganic chemicals of interest. The infrared absorption bands specify the special molecular ingredient or structures, and provide chemical bonding information of the materials because of the vibrational movements of the chemical bond showing frequencies in the infrared spectrum (Ojeda & Dittrich, 2012).

In this study, chemical composition of the deposited coatings was analyzed by Fourier Transform Infrared Spectroscopy (FTIR, Perkin Elmer Spectrum BX) with a spectral range of 650-4000 cm^{-1}.

4.5.4 Electrochemical Method

In this study, the corrosion mesaurement was applied using a Gamry potentiostat/galvanostat system operated by the Gamry Framework and Echem Analyst software, for the obtain and analysis of electrochemical data, respectively. Electrochemical characterization was carried out by potentiodynamic measurements in order to measure corrosion behavior of the obtained coatings. Corrosion tests were applied at 25±1°C in %5 NaCl solution.

Measurement of the open circuit potential (OCP) was applied in the test suspension for 30 minutes. The potentiodynamic graphs were collected sweeping potential from -1V vs OCP to 2V vs Saturated calomel electrode with 0.5mV/s scan rate.

CHAPTER FIVE
RESULTS AND DISCUSSION

5.1 Electrolyte Analysis

The electrical conductivities, pH values, zeta potentials and average size of the suspensions are givent at Table 5.1. Results show that addition of dispersant results in decrement of average size of particles and increasement of zeta potential, conductivity and pH.

Table 5.1 pH, conductivity values, zeta potential and average size values of suspensions

Suspension		pH	Conductivity Value (µS/cm)	Zeta Potential (mV)	Avarage Size (nm)
HAP (g/l)	DEA (g/l)				
40	0	6.95	0.07	4.73	1360
40	2	9.11	0.19	5.91	831.8
40	6	10.72	0.31	6.23	792.8
40	10	10.89	0.39	6.59	733.5

Zeta potential is the key factor in EPD technique. It plays major role for stabilization of the suspension by repulse interaction between particles and also it determines the particle movement direction during the deposition process. The charged particles are surrounded by ions and the concetration of the ion is higher near paticle surface and it decreases as the distance increases. Such kind of ion distribution forms and electrical double layer shown in Figure 5.1. The Electrical double layer consist of stern layer, diffuse layer and sperated by Helmholtz plane. Stern layer is located near the particle surface. Generally, a particle with negative surface shows a positive zeta potential. This potential gives the degree of repulsion between adjacent and similarly charged powders in the dispersion. High zeta potential shows that the colloidal dispersion is stable and if the zeta potential is low it shows the repulsion and dispersion will break and coagulate (Besra & Liu, 2007).

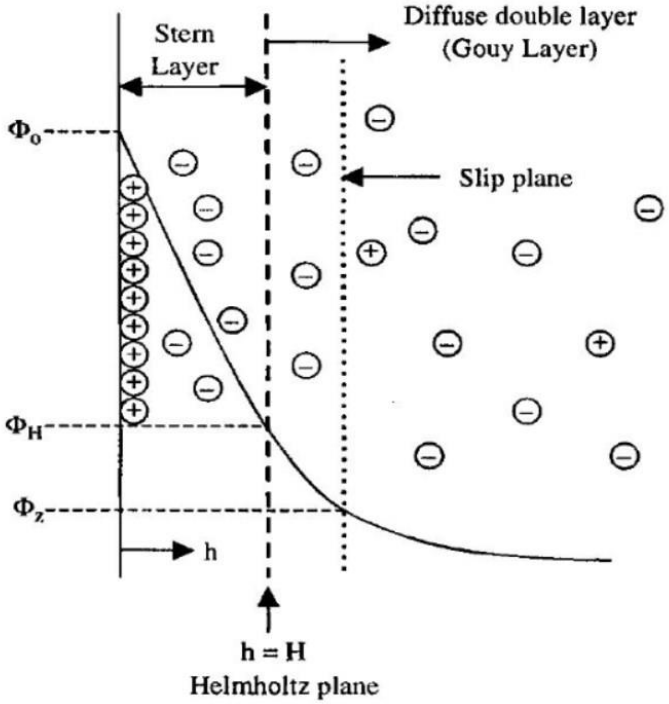

Figure 5.1 Structure of double layer and distribution of potential

pH is also key point for EPD process. At the same time different parameters are related with each other in the EPD process. Figure 5.2 shows the combinatorial effect of zeta potential and electric conductivity of the solution. It can be seen from the Figure 5.2 shows that pH value reduces from 7.5 to 4.5, the zeta potential value improves. This is due to adsorption of Hydrogen ions on powder surfaces which increases the electrostatic repulsion force and the zeta potential value increases. But pH at very low from 4.5 to 2.0 large amount of positive ions reduce double layer thickness. Because of repulsive force between the particles also gets decreased and also it leads to particle agglomeration (Besra & Liu, 2007).

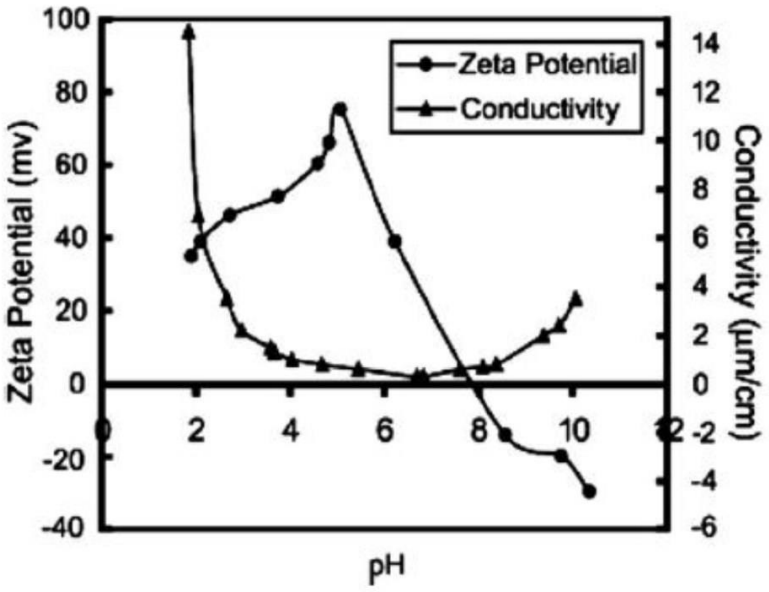

Figure 5.2 Zeta potential and conductivity value with varying pH in aqueous media (Besra & Liu, 2007)

Thus, high ionic concentration, agglomeration increases and this situation handicap for mobility of powder so electrical conductivity of solution directly influences (Powers, 1975).

Selecting suspension parameters needs to be given more attention to get a high quality EPD depositon for coating CaP.

The zeta potential and the colloidal steady of powders can be increased by the addition of an efficient dispersant into the suspensions (Farrokhi-Rad & Shahrabi, 2013).

In this study DEA can be utilized as the dispersant to improve the zeta potential value and colloidal steady of powders in butanol. Shahrabi et al. found the similar zeta potential results in their research with isopropanol. (Farrokhi-Rad & Shahrabi, 2013).

5.2 Phase Analysis

The XRD patterns of depositied Ti6Al4V alloy substrates after heat treatment process are shown in from Figure 5.3 to Figure 5.4.All coatings are composed of HAP phase according to JCPDS 09-0432. Besides, diffraction peaks of Ti (JCPDS 044-1294) arise from substrate.

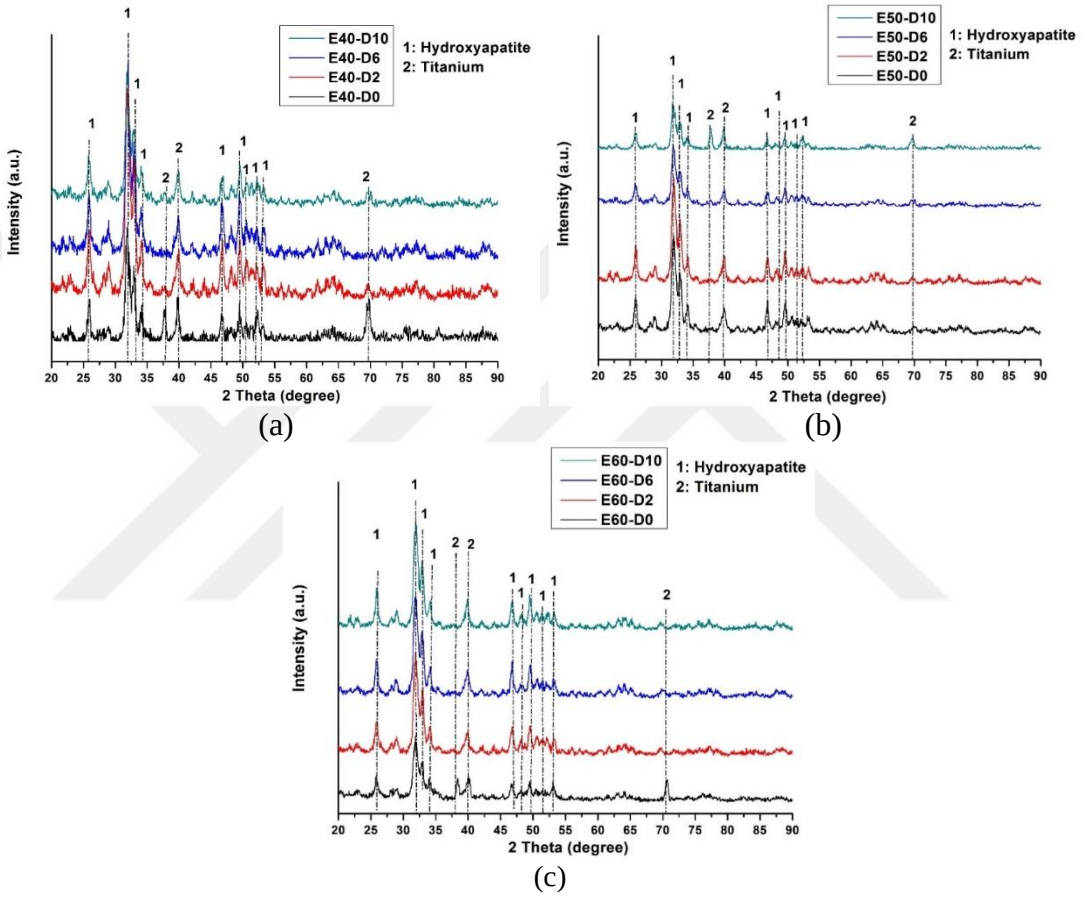

Figure 5.3 XRD spectrum of coatings deposited at (a) 40V, (b) 50V and (c) 60 V applied voltage with 2-6-10 g/l DEA

The X-ray patterns of the coatings at 40V, 50 V and 60 V applied voltage values are shown in Figure 5.3 with increasing amount of DEA dispersant. Results of coatings deposited without DEA are also given for comparison. It is observed that there was not any significant difference in coating phase structure with different amounts of dispersant.

The X-ray patterns of the coatings at 40 V, 50 V and 60 V applied voltages by using a suspension including 10g/l DEA are shown in Figure 5.4 in order to research the effect of carried out voltage for coating with constant amount of DEA. It was observed that there was no major change in coating phase structure with varying voltage with 10g/l DEA.

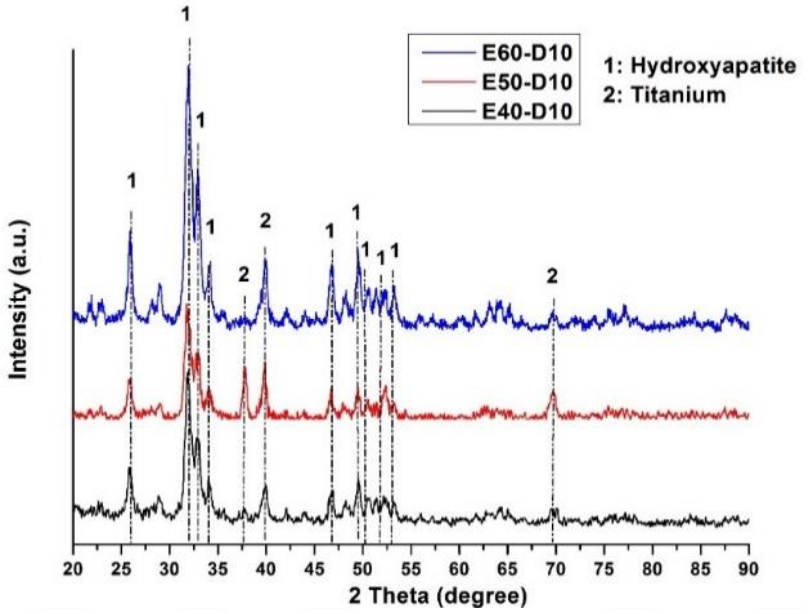

Figure 5.4 XRD patterns of coatings at 40-50-60V applied voltages with a suspension including 10 g/l DEA

X-ray diffraction technique gives a peak for crystalline material (Artioli, 1999). As a result, DEA is an organic compound, not have the crystalline structure so neither the amount of DEA dispersant nor the applied voltage value during deposition process do not altered the phase structure of deposited coatings.

5.3 FTIR Analysis

The FTIR spectra patterns of coated samples on Ti6Al4V alloys substrates after heat treatment process are shown in from Figure 5.5 to Figure 5.6. According to the FTIR spectra, all bands between 960 and 1100 cm^{-1} (1100 cm^{-1}, 1030 cm^{-1} and 960 cm^{-1}) are attributed to characteristic peak due to the PO_4^{3-} in HAP (Park & Lakes,

2007). The band at 3400 cm^{-1} is assigned to OH stretching of H_2O (Barrere, van Blitterswijk, De Groot, & Layrolle, 2002).

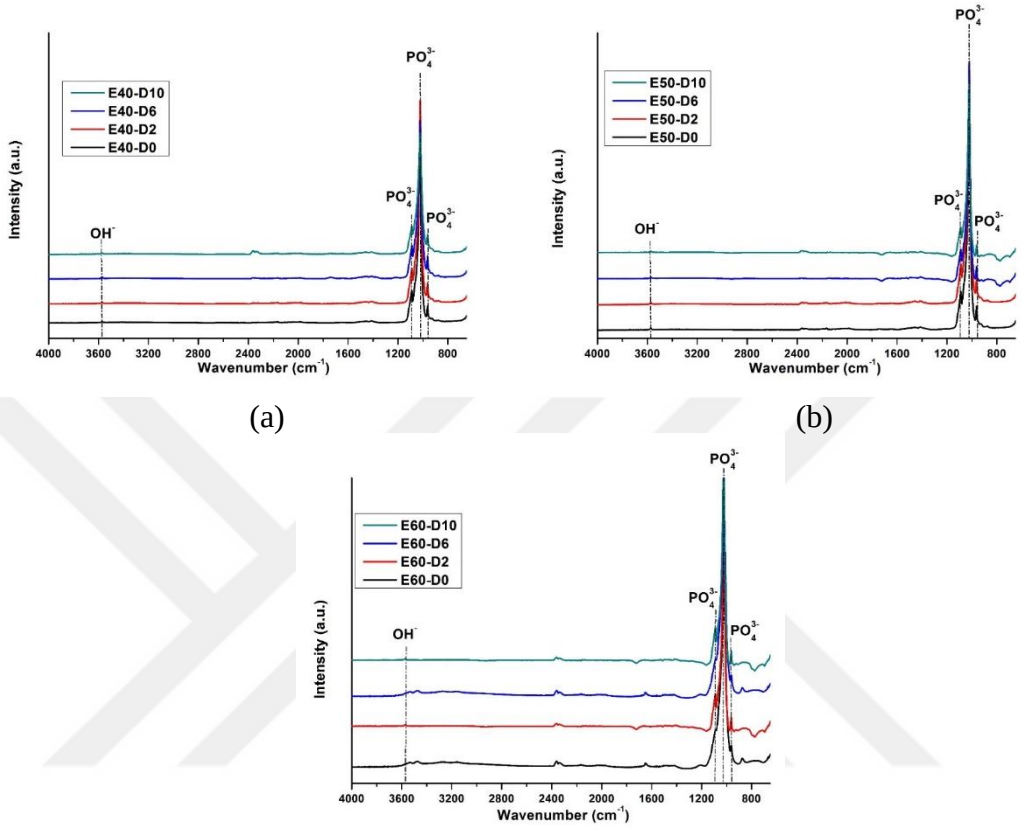

Figure 5.5 FTIR spectra of coatings deposited at (a) 40V, (b) 50V and (c) 60 V applied voltage with 0-2-6-10 g/l DEA

The FTIR spectra of the coatings deposited at 40V, 50 V and 60 V applied voltage values are shown in Figure 5.5 with increasing amount of DEA dispersant. Results of coatings deposited without DEA are also given for comparison. It is observed that there was not any major difference in coating spectra structure with different amounts of dispersant.

The FTIR spectra of the coatings at 40 V, 50 V and 60 V applied voltages by using a suspension including 10g/l DEA are shown in Figure 5.6 in order to research the effect of applied voltage for deposition with constant amount of DEA. It was observed

that there was no major change in coating spectra structure with varying voltage with 10g/l DEA.

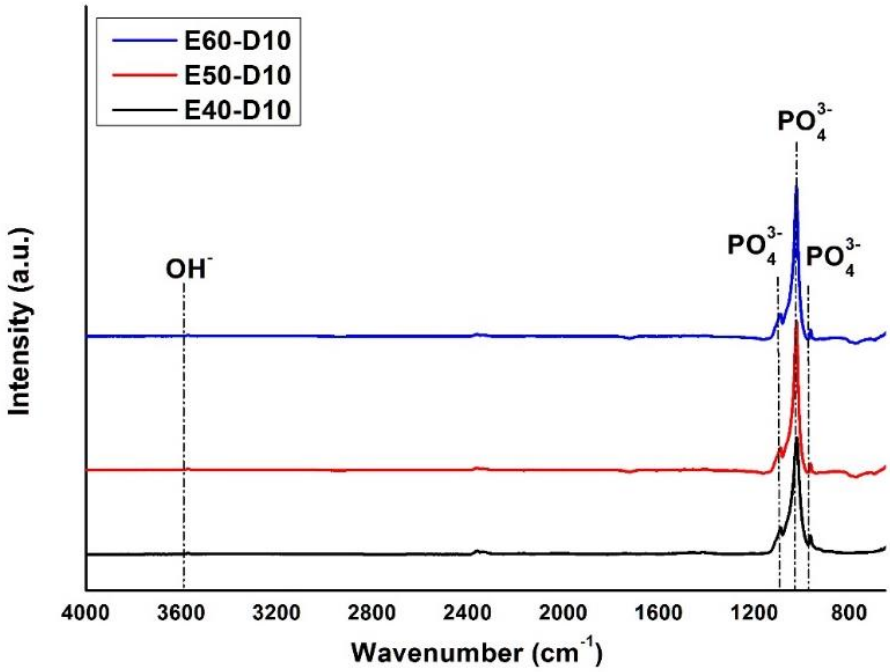

Figure 5.6 FTIR spectra for 10g/l DEA with 40-50-60V samples E40-D10, E50-D10, E60-D10

Organic dispersants characteristics peaks at 2875 and 2945 cm^{-1} (Farrokhi-Rad & Shahrabi, 2013) but according to FTIR spectrum increasing of DEA could not change the spectrum because of organic compound DEA removed after heat treatment.

As a result, neither the amount of DEA dispersant nor the applied voltage value during deposition process do not altered the spectra structure of deposited coatings because of sintering.

5.4 Scanning Electron Microscope Analysis

The surface morphologies of coated samples on Ti6Al4V alloys substrates after heat treatment process are shown in from Figure 5.7 to Figure 5.11.

The surface morphologies of the 40V samples with 0-2-60-10 g/l DEA are shown in Figure 5.7. It was observed that crack formation decreasing as increasing of the DEA for 40 V samples. Figure 5.7 shows the coatings deposited from the suspension with 0, 2 and 6 g/l DEA for 40V have the high concentrations of large fractures and

cracks developed during drying afer coatings. The coating deposited from the suspension with 10 g/l DEA has smaller cracks. Cracks forming in EPD coating due to drying shrinkages. (Besra & Liu, 2007; Farrokhi-Rad & Shahrabi, 2013). Because of drying shrinkages makes stress on the coatings and after cracks formation on the coating.

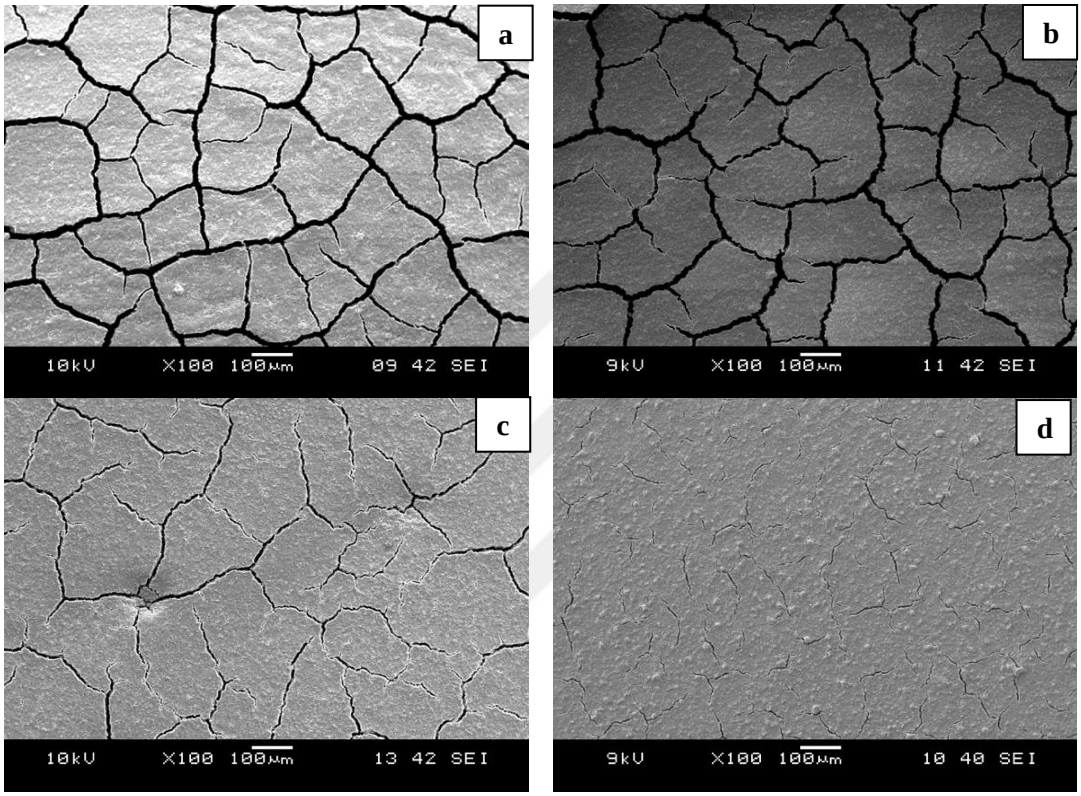

Figure 5.7 SEM images of the 40V samples with 0-2-6-10 g/l DEA at 100x magnification; (a) E40-D0, (b) E40-D2, (c) E40-D6, (d) E40-D10

The surface morphologies of the 50V samples with 0-2-60-10 g/l DEA are shown in Figure 5.8. It was observed that crack formation decreasing as increasing of the DEA for 50 V samples. Figure 5.8 shows the coatings deposited from the suspension with 0 and 2 g/l DEA for 50V have the high concentrations of large cracks occured during drying afer depositions due to drying shrinkages. The coating deposited from the suspension with 6 and 10 g/l DEA have smaller cracks.

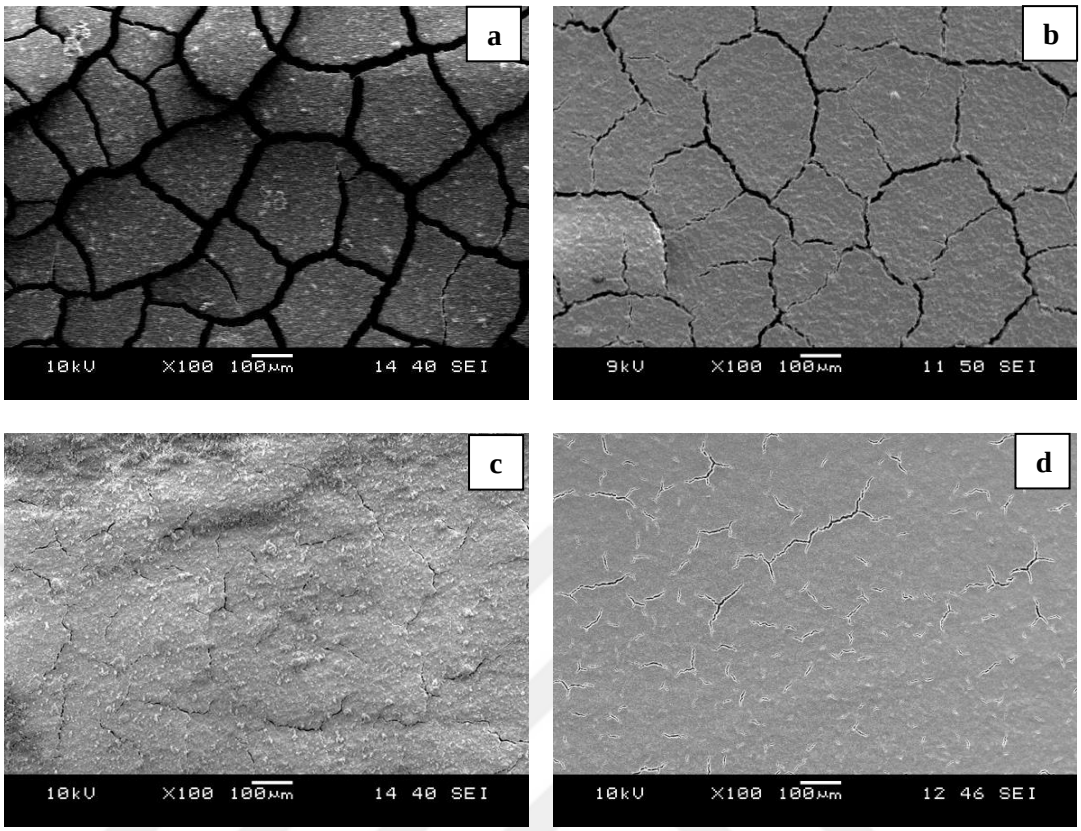

Figure 5.8 SEM images of the 50V samples with 0-2-6-10 g/l DEA at 100x magnification; (a) E50-D0, (b) E50-D2, (c) E50-D6, (d) E50-D10

The surface morphologies of the 60V samples with 0-2-60-10 g/l DEA are shown in Figure 5.9. It was observed that crack formation decreasing as increasing of the DEA for 60 V samples. Figure 5.9 shows the coatings deposited from the suspension with 0 g/l DEA for 60V have the high concentrations of large cracks occured during drying afer coatings due to drying shrinkages and 2 g/l DEA coatings smaller than 0 g/l DEA. The coating deposited from the suspension with 6 and 10 g/l DEA have no cracks.

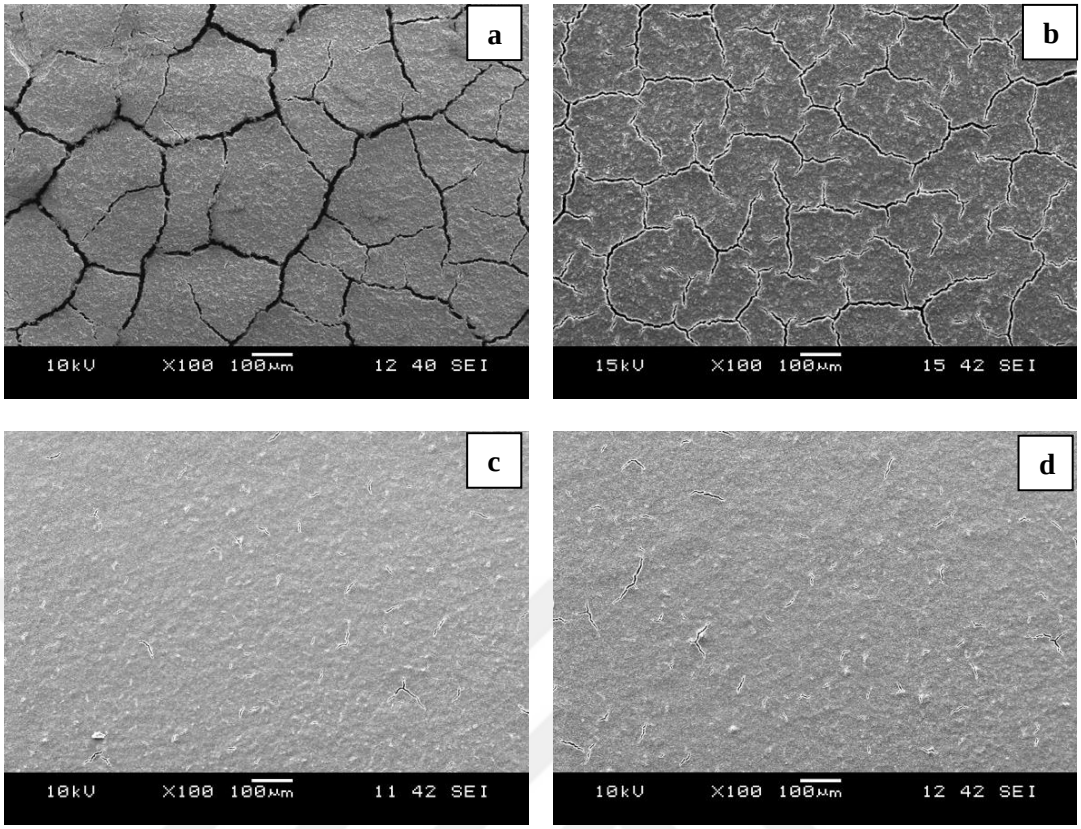

Figure 5.9 SEM images of the 60V samples with 0-2-6-10 g/l DEA at 100x magnification; (a) E60-D0, (b) E60-D2, (c) E60-D6, (d) E60-D10

The surface morphologies of the 10 g/l DEA samples with 40-50-60 V are shown in Figure 5.10. It was observed that crack formation decreasing as increasing of the voltage for 10 g/l DEA samples. Figure 5.10 shows cracking does not develop in the coatings deposited from the suspension with 10 g/l wih 60 V. This sample can be tolerate the drying shrinkages stress on coatings and no cracks occurring.

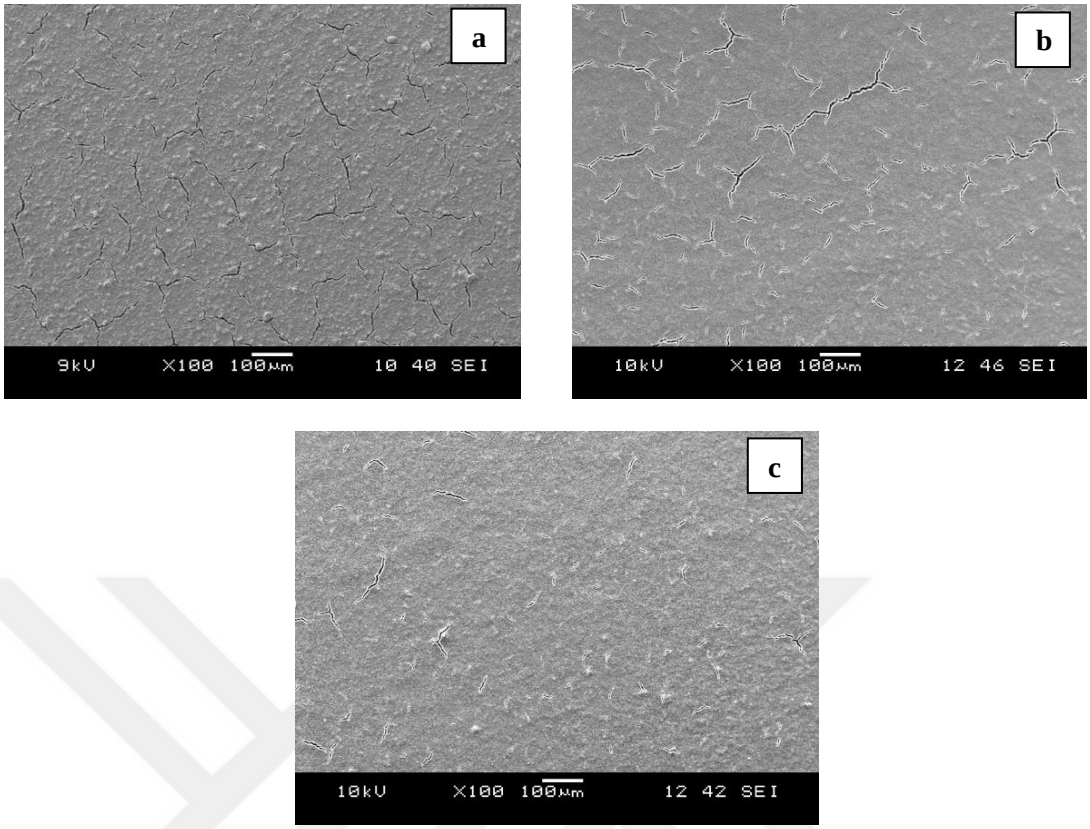

Figure 5.10 SEM images of the 10 g/l DEA samples with 40-50-60V at 100x magnification; (a) E40-D10, (b) E50-D10, (c) E60-D10

The surface morphologies of the 60V samples with 0-2-60-10 g/l DEA at higher magnification (X5000) presented in Figure 5.11.

DEA addition has microstructure with fine particles and small number of agglomerates. However in the coatings especially produced without the use of dispersant have rough microstructure with coarse agglomerated particles. As can be seen among the coatings, the one coated from the solution with 10g/l has the best microstructure wih fine particles and small number of fine agglomerates. However other coatings, especially coated from the suspension with 0 and 2 g/l, have unstable microstructures with coarse agglomerates.

The zeta potential of suspension is the highest (6.59 mV) with 10g/l DEA; thus the particles agglomeration is small in it due to large reoulsion electrostatic force between them. These SEM results were similiar to that reported by Shahrabi et. al. (Besra & Liu, 2007; Farrokhi-Rad & Shahrabi, 2013)

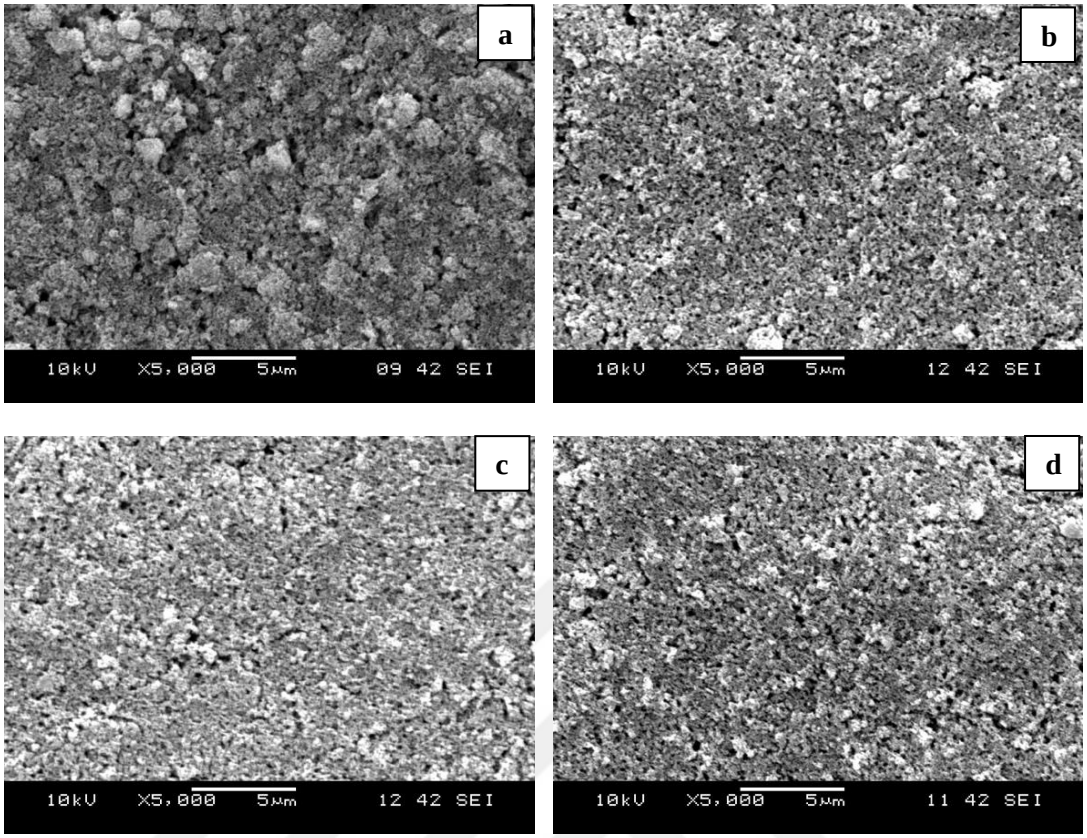

Figure 5.11 SEM images of the 60V samples with 0-2-6-10 g/l DEA at 5000x magnification; (a) E60-D0, (b) E60-D2, (c) E60-D6, (d) E60-D10

The Ca/P molar ratios of the all samples calculated from the EDS analyses and for all samples were changed in range from 1.72 to 1.78 and these values are close to the ratio of hydroxyapatite (Besra & Liu, 2007). This results also confirmed by XRD and FTIR analyses.

5.5 Electrochemical Characterization

The Potentiodynamic polarization curves obtained from coated samples on Ti6Al4V alloys substrates after heat treatment process are shown in from Figure 5.12 to Figure 5.15.

Electrochemical spesifications of the corrosion potential (E_{cor}) and corrosion current density (I_{cor}) values obtained from coated samples on Ti6Al4V alloys substrates after heat treatment process are shown in from Table 5.2 to Table 5.6.

Figure 5.12 shows potentiodynamic polarization behaviour of etched 40V coatings with 0-2-6-10g/l DEA. Results show that the corrosion resistance of 10g/l DEA etched 40V coatings has significantly improved compared to without DEA coatings.

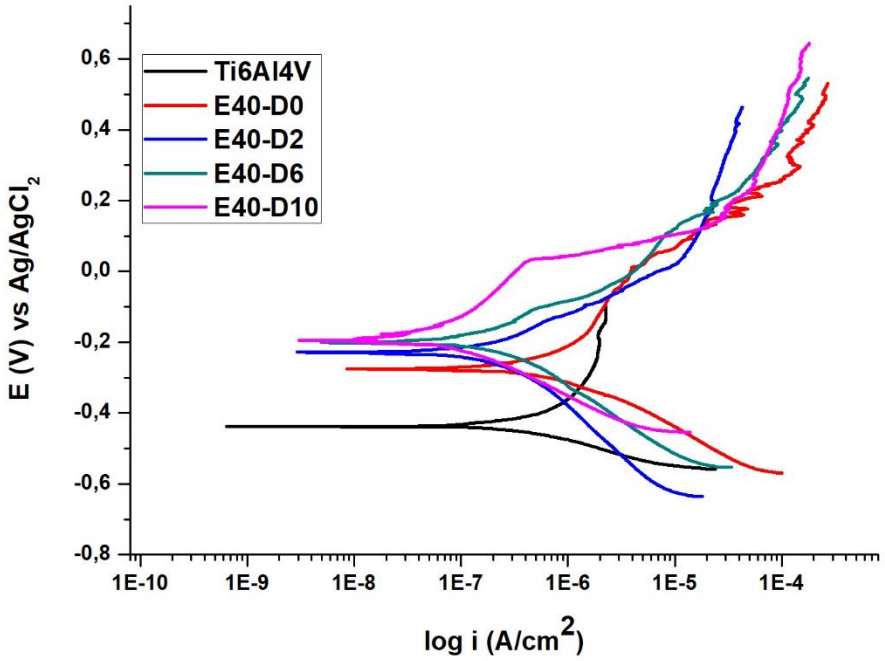

Figure 5.12 Potentiodynamic polarization results of 40V coatings

Tafel extrapolation method and results are showed in Table 5.2 for 40 V samples with 0-2-6-10g/l DEA. Increasing of DEA concentration decreases I_{cor} of the sample from 201.62 nA to 141 nA. According to I_{cor}, the corrosion resistance of the 40V samples are ranked as: E40-D10 > E40-D6 > E40-D2 > E40-D0 > Ti6Al4V.

Table 5.2 Electrochemical results of the Ti6Al4V substrate and 40V coatings

Specimen	E_{cor} (V)	I_{cor} (nA)
Ti6Al4V	-0,434	314.63
E40-D0	-0.274	201.62
E40-D2	-0.227	173.21
E40-D6	-0.200	151.13
E40-D10	-0.194	141

Figure 5.13 shows potentiodynamic polarization behaviour of etched 50V coatings with 0-2-6-10g/l DEA. Results show that the corrosion resistance of 10g/l DEA etched 50V coatings has significantly improved compared to without DEA coatings.

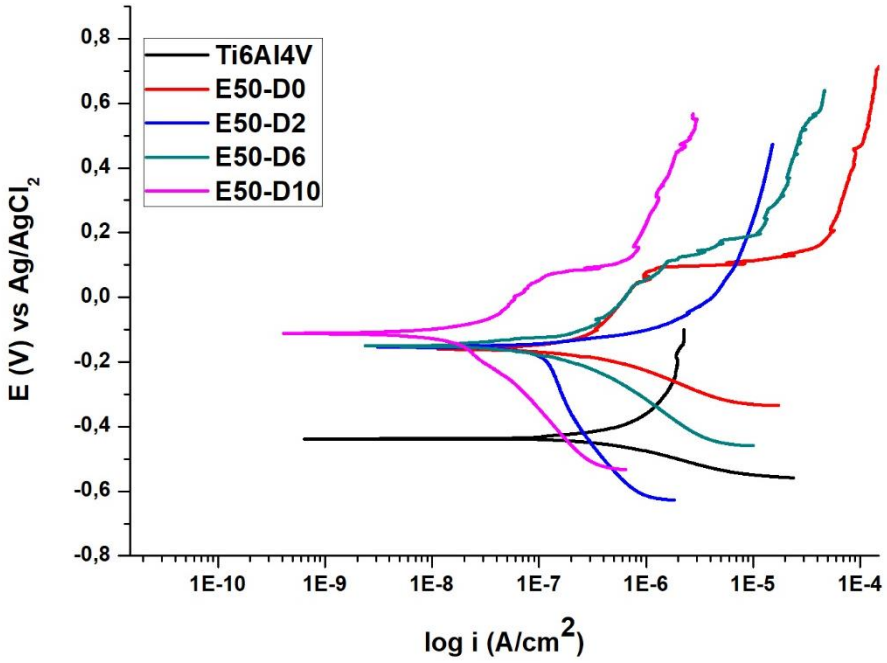

Figure 5.13 Potentiodynamic polarization results of 50V coatings

Tafel extrapolation method and results are showed in Table 5.3 for 50 V samples with 0-2-6-10g/l DEA. Increasing of DEA concentration decreases I_{cor} of the sample from 119.91 nA to 80.16 nA. According to I_{cor}, the corrosion resistance of the 50V samples are ranked as: E50-D10 > E50-D6 > E50-D2 > E50-D0 > Ti6Al4V.

Table 5.3 Electrochemical results of the Ti6Al4V substrate and 50V coatings

Specimen	E_{cor} (V)	I_{cor} (nA)
Ti6Al4V	-0,434	314.63
E50-D0	-0.159	119.91
E50-D2	-0.152	116.31
E50-D6	-0.150	111.63
E50-D10	-0.111	80.16

Figure 5.14 shows potentiodynamic polarization behaviour of etched 60V coatings with 0-2-6-10g/l DEA. Results show that the corrosion resistance of 10g/l DEA etched 60V coatings has significantly improved compared to without DEA coatings.

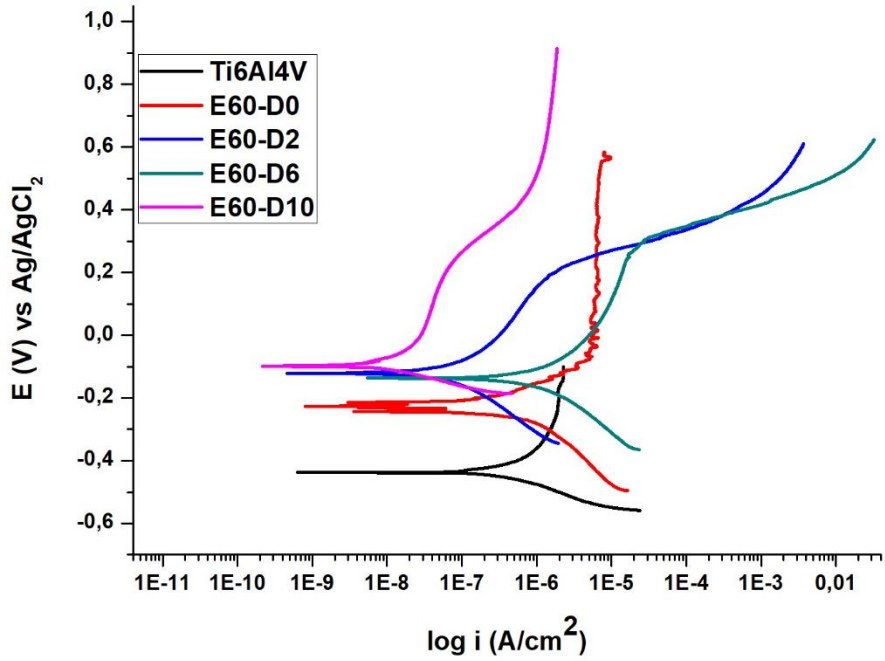

Figure 5.14 Potentiodynamic polarization results of 60V coatings

Tafel extrapolation method and results are showed in Table 5.4 for 60 V samples with 0-2-6-10g/l DEA. Increasing of DEA concentration decreases I_{cor} of the sample from 179.51 nA to 69.17 nA. According to I_{cor}, the corrosion resistance of the 60V samples are ranked as: E60-D10 > E60-D6 > E60-D2 > E60-D0 > Ti6Al4V.

Table 5.4 Electrochemical results of the Ti6Al4V substrate and 60V coatings

Specimen	E_{cor} (V)	I_{cor} (nA)
Ti6Al4V	-0,434	314.63
E60-D0	-0,248	179.51
E60-D2	-0,113	94.29
E60-D6	-0,129	113.05
E60-D10	-0,097	69.17

Figure 5.15 shows potentiodynamic polarization behaviour of 10 g/l DEA coatings with 40-50-60 V. Results show that the corrosion resistance of 60V with 10g/l DEA

coatings has significantly improved compared to 40 and 50 V coatings with 10 g/l DEA.

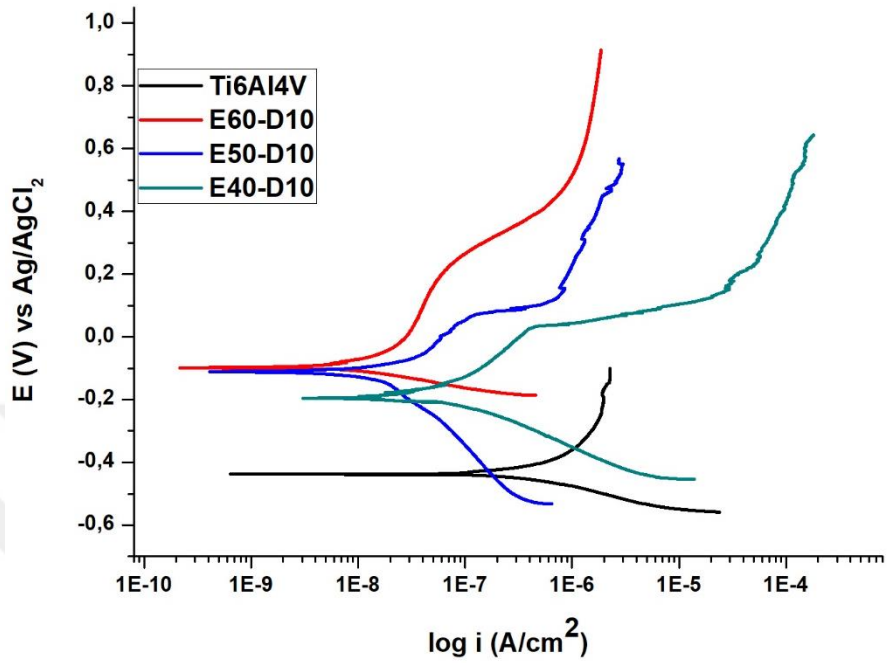

Figure 5.15 Potentiodynamic polarization results of 10g/l DEA coatings

Tafel extrapolation method and results are showed in Table 5.5 for 10 g/l DEA samples with 40-50-60 V. Increasing of Voltage decreases I_{cor} of the sample from 141 nA to 69.17 nA. According to I_{cor}, the corrosion resistance of the 10 g/l DEA samples are ranked as: E60-D10 > E50-D10 > E40-D10 > Ti6Al4V.

Table 5.5 Electrochemical results of the Ti6Al4V substrate and 10g/l DEA coatings

Specimen	**E_{cor} (V)**	**I_{cor} (nA)**
Ti6Al4V	-0.434	314.63
E40-D10	-0.194	141
E50-D10	-0.111	80.16
E60-D10	-0.097	69.17

CHAPTER SIX
CONCLUSION

6.1 General Results

CaP were successfully coated on Ti6Al4V substrates via electrophoretic deposition technique. The effect of diethanolamine dispersant, coating time and surface treatment of Ti6Al4V alloy was investigated on structural properties of coatings. The properties of suspensions were analysed by pH, conductivity, Zeta potential, particle size. The properties of coatings were characterized by SEM and electrochemical analysis.

According to XRD and FTIR analyses all coatings are composed of HAP and a significant change was not observed with using dispersant.

According to FTIR spectrum increasing of DEA could not change the spectrum because of organic compound DEA removed during sintering. Some dispersants in biomedical applications cause toxic or adverse to the cells (Zhitomirsky & Gal-Or, 1997). Thus, this toxicity risk is eliminated with heat treatment.

According to SEM images morphology of coatings produced by using HAP suspension with DEA addition are crack-free and more homogenous in comparison to coatings produced by using HAP suspension with DEA addition.

DEA dispersant has made a distinct change at surface morphology of the coatings due to the pH, zeta potential and conductivity increment of the suspension. As result, particles was repulsed each other, agglomeration of particles were decreased and the stability of suspension changed.

This is probably due to the increment of pH value of suspension with usage of dispersant. The increment of the pH causes a great amount of positive ion to increase, which also causes the increment of the thickness of the double layer. Thus, the particles start to repulse each other; and this decrease the amount of agglomerated particles. Accordingly, the size distribution of particles in suspension decreases. Consequently, with the formation of homogeneous suspension, electrical conductivity increases. This

results were similiar to that reported by Besra et. al. and Shahrabi et. al. (Besra & Liu, 2007; Farrokhi-Rad & Shahrabi, 2013).

HAP suspension with DEA addition has the highest zeta potential, due to the particle agglomeration is small in it due to the large repulsion electrostatic between particles with increment of DEA Shahrabi et al. found equivalent conclusion in their research (Farrokhi-Rad & Shahrabi, 2013).

Also it was found that the coating with 60V, 10 g/l DEA had the best corrosion resistance because of its fine, homogenous and crack free stable morphologhy was acted as a good barrier against corrosive medium.

In conclusion it was found that HAP-DEA suspension leads to homogeneous and crack-free microstructure due to the highest zeta potential and better colloidal stability in comparison to the HAP suspension .

REFERENCES

Agarwal, R., & García, A. J. (2019). Surface modification of biomaterials, *Principles of Regenerative Medicine* (651-660). London:Elsevier.

Agrawal, C. M. (1998). Reconstructing the human body using biomaterials. *Jom, 50* (1), 31-35.

Aherwar, A., Singh, A. K., & Patnaik, A. (2016). Cobalt based alloy: a better choice biomaterial for hip implants. *Trends in Biomaterials & Artificial Organs, 30* (1) 66-69.

Ahmed, W., Jackson, M. J., & Jackson, M. J. (2009). *Emerging nanotechnologies for manufacturing*: New York:William Andrew.

Aliofkhazraei, M., Ali, N., Milne, W. I., Ozkan, C. S., Mitura, S., & Gervasoni, J. L. (2016). Graphene Science Handbook, Six-Volume Set. Florida:Crc Press.

Amrollahi, P., Krasinski, J. S., Vaidyanathan, R., Tayebi, L., & Vashaee, D. (2016). Electrophoretic deposition (EPD): Fundamentals and applications from nano-to micro-scale structures. *Handbook of nanoelectrochemistry: electrochemical synthesis methods, properties and characterization Techniques*, 1-27.

Artioli, G. (1999). *Inorganic compounds and minerals studied using X-ray diffraction*. London:Elsevier

Augello, C., & Liu, H. (2015). Surface modification of magnesium by functional polymer coatings for neural applications *Surface Modification of Magnesium and its Alloys for Biomedical Applications* (335-353). London:Elsevier.

Avcu, E., Baştan, F. E., Abdullah, H. Z., Rehman, M. A. U., Avcu, Y. Y., & Boccaccini, A. R. (2019). Electrophoretic deposition of chitosan-based composite

coatings for biomedical applications: A Review. *Progress in Materials Science*, *103*, 69-108.

Azem, F. A., Eroglu, E., & Cakir, A. (2011). Synthesis and structural properties of sol-gel derived Si-substituted hydroxyapatite coatings. *Journal of Biomechanics, 44*(1), 13.

Baino, F., Novajra, G., & Vitale-Brovarone, C. (2015). Bioceramics and scaffolds: a winning combination for tissue engineering. *Frontiers in Bioengineering and Biotechnology*, *3*, 202.

Barrere, F., van Blitterswijk, C. d., De Groot, K., & Layrolle, P. (2002). Influence of ionic strength and carbonate on the Ca-P coating formation from SBF× 5 solution. *Biomaterials*, *23* (9), 1921-1930.

Besra, L., & Liu, M. (2007). A review on fundamentals and applications of electrophoretic deposition (EPD). *Progress in Materials Science*, *52* (1), 1-61.

Bir, F., Khireddine, H., Touati, A., Sidane, D., Yala, S., & Oudadesse, H. (2012). Electrochemical depositions of fluorohydroxyapatite doped by Cu2+, Zn2+, Ag+ on stainless steel substrates. *Applied Surface Science*, *258* (18), 7021-7030.

Blau, P. J. (1992). Friction, lubrication, and wear technology. *ASM International*, 175-235 Ohio:ASM International Society.

Boccaccini, A., Keim, S., Ma, R., Li, Y., & Zhitomirsky, I. (2010). Electrophoretic deposition of biomaterials. *Journal of the Royal Society Interface*, *7*, 581-613.

Bordjih, K., Jouzeau, J.-Y., Mainard, D., Payan, E., Delagoutte, J.-P., & Netter, P. (1996). Evaluation of the effect of three surface treatments on the biocompatibility of 316L stainless steel using human differentiated cells. *Biomaterials*, *17*(5), 491-500.

Bosco, R., Van Den Beucken, J., Leeuwenburgh, S., & Jansen, J. (2012). Surface engineering for bone implants: a trend from passive to active surfaces. *Coatings*, *2*(3), 95-119.

Bronzino, J. D., Wong, J. Y., & Peterson, D. R. (2012). B*iomaterials: Principles and Practices*. Florida:CRC Press.

Brunette, D. M., Tengvall, P., Textor, M., & Thomsen, P. (2012). *Titanium in medicine: material science, surface science, engineering, biological responses and medical applications*. Berlin:Springer Science & Business Media.

Callister Jr, W. D., & Rethwisch, D. G. (2012). *Fundamentals of materials science and engineering: an integrated approach*. New Jersey: John Wiley & Sons.

Chen, Q., & Thouas, G. (2014). *Biomaterials: a basic introduction.* Florida: CRC Press.

Cheng, K., Wang, T., Weng, W., Yu, M., Lin, J., Wang, H., Han, G. (2013). Two step synthesis of CaP/TiO2 nanorod composite coatings with improved protein adsorption. *Thin Solid Films, 544*, 206-211.

Chhetri, S., Kuila, T., & Murmu, N. C. (2016). Graphene Composites. *Graphene Technology: From Laboratory to Fabrication*, 63-111.

Cordelair, J., & Greil, P. (2004). Discrete element modeling of solid formation during electrophoretic deposition. *Journal of Materials Science*, *39*(3), 1017-1021.

Davis, J. *Handbook of Materials for Medical Devices*. (2003). Ohio: ASM International Google Scholar

Davis, J. (2003). Overview of biomaterials and their use in medical devices. *Handbook of materials for medical devices*, 1-11.

De Aza, P., Guitian, F., Santos, C., De Aza, S., Cusco, R., & Artus, L. (1997). Vibrational properties of calcium phosphate compounds. 2. Comparison between hydroxyapatite and β-tricalcium phosphate. *Chemistry of Materials*, *9*(4), 916-922.

Donglu, S. (2005). *Introduction to biomaterials.* Singapore:World Scientific.

Dorozhkin, S. V. (2012). *Calcium orthophosphates: applications in nature, biology, and medicine.* Singapore:Pan Stanford.

Dorozhkin, S. V., & Epple, M. (2002). Biological and medical significance of calcium phosphates. *Angewandte Chemie International Edition*, *41*(17), 3130-3146.

Ducheyne, P., Radin, S., Heughebaert, M., & Heughebaert, J. (1990). Calcium phosphate ceramic coatings on porous titanium: effect of structure and composition on electrophoretic deposition, vacuum sintering and in vitro dissolution. *Biomaterials*, *11*(4), 244-254.

Esfehanian, M., Raissi-Dehkordi, B., & Moztarzadeh, F. (2005). Electrophoretic deposition of hydroxyapatite on metal implants. *Interceram*, *54*(2), 92-98.

Farrokhi-Rad, M., & Shahrabi, T. (2013). Effect of triethanolamine on the electrophoretic deposition of hydroxyapatite nanoparticles in isopropanol. *Ceramics International*, *39*(6), 7007-7013.

Fedotkin, A., Bolbasov, E., Kozelskaya, A., Dubinenko, G., Shesterikov, E., Ashrafov, A., & Tverdokhlebov, S. (2019). Calcium phosphate coating deposition by radio frequency magnetron sputtering in the various inert gases: The pilot study. *Materials Chemistry and Physics*, *40* (6), 121-735.

Filiâtre, C., Pignolet, C., & Buron, C. (2017). Particle Velocities near and along the Electrode during Electrophoretic Deposition: Influence of Surfactant Counter-Ions. *Coatings*, *7*(9), 147-162.

Guo, M., Fang, H., Wang, R., Yang, Z., & Xu, X. (2011). Electrodeposition of chitosan-glucose oxidase biocomposite onto Pt–Pb nanoparticles modified stainless steel needle electrode for amperometric glucose biosensor. J*ournal of Materials Science: Materials in Medicine*, *22*(8), 1985-1992.

Habibovic, P., Barrere, F., Van Blitterswijk, C. A., de Groot, K., & Layrolle, P. (2002). Biomimetic hydroxyapatite coating on metal implants. *Journal of the American Ceramic Society*, *85*(3), 517-522.

Harun, W. S. W., Asri, R. I. M., Sulong, A. B., Ghani, S. A. C., & Ghazalli, Z. (2018). Hydroxyapatite-Based Coating on Biomedical Implant. *Hydroxyapatite: Advances in Composite Nanomaterials, Biomedical Applications and Its Technological Facets.* Zagreb:Intechopen.

Heimke, G., & Stock, D. (1984). Clinical application of ceramic osseo–or soft tissue-inte-grated implant. *Orthopaedic Ceramic Implants*, *4*, 1-19.

Helmersson, U., Lattemann, M., Bohlmark, J., Ehiasarian, A. P., & Gudmundsson, J. T. (2006). Ionized physical vapor deposition (IPVD): A review of technology and applications. *Thin Solid Films*, *513*(1-2), 1-24.

Heughebaert, J.-C., Zawacki, S. J., & Nancollas, G. H. (1983). The growth of octacalcium phosphate on beta tricalcium phosphate. *Journal of Crystal Growth*, *63*(1), 83-90.

Huang, S., Zhou, K., Huang, B., Li, Z., Zhu, S., & Wang, G. (2008). Preparation of an electrodeposited hydroxyapatite coating on titanium substrate suitable for in-vivo applications. J*ournal of Materials Science: Materials in Medicine*, *19*(1), 437-442.

International, A. (2003). Handbook of materials for medical devices. Ohio:ASM international.

Jansen, J. A., & Leon, B. (2009). *Thin calcium phosphate coatings for medical implants*. Berlin:Springer.

Kamminga, M. E., Gélvez-Rueda, M. C., Maheshwari, S., van Droffelaar, I. S., Baas, J., Blake, G. R., Palstra, T. T. (2019). Electronic mobility and crystal structures of 2, 5-dimethylanilinium triiodide and tin-based organic-inorganic hybrid compounds. *Journal of Solid State Chemistry*, *270*, 593-600.

Kelly, P. J., & Arnell, R. D. (2000). Magnetron sputtering: a review of recent developments and applications. *Vacuum*, *56*(3), 159-172.

Kowalchuk, R. M., Pollack, S. R., Ducheyne, P., & King, L. A. (1993). Particle microelectrophoresis of calcium-deficient hydroxyapatite: solution composition and kinetic effects. *Journal of Biomedical Materials Research*, *27*(6), 783-790.

Kwok, C., Wong, P., Cheng, F., & Man, H. (2009). Characterization and corrosion behavior of hydroxyapatite coatings on Ti6Al4V fabricated by electrophoretic deposition. *Applied Surface Science*, *255*(13-14), 6736-6744.

Larsson, M., Hill, A., & Duffy, J. (2012). Suspension stability; why particle size, zeta potential and rheology are important. *Nordic Rheology Society*, *20*, 209-214.

Levingstone, T. J., Ardhaoui, M., Benyounis, K., Looney, L., & Stokes, J. T. (2015). Plasma sprayed hydroxyapatite coatings: Understanding process relationships using design of experiment analysis. *Surface and Coatings Technology*, *283*, 29-36.

Levitus, S., & Boyer, T. P. (1994). *World ocean atlas 1994. volume 4. temperature*. Washington:Osti

Li, S.-T., Park, J., & Bronzino, J. (2003). Biomaterials: Principles and Applications. *Eds. JB Park, JOS Bronzino-Boca Raton.* Florida: SRC Press LLC, 115-139.

Liu, C., Zhang, J., Zhang, S., Wang, P., Lian, Y., Deng, S., & He, Y. (2017). Preparation and properties of ceramic coatings by cathode plasma electrolytic deposition on titanium alloy. *Surface and Coatings Technology*, *325*, 708-714.

Long, J., Xu, S., Cai, J., Jiang, N., Lu, J., Ostrikov, K., & Diong, C. (2002). Structure, bonding state and in-vitro study of Ca–P–Ti film deposited on Ti6Al4V by RF magnetron sputtering. *Materials Science and Engineering: C*, *20*(1-2), 175-180.

Ma, Y., Han, J., Wang, M., Chen, X., & Jia, S. (2018). Electrophoretic deposition of graphene-based materials: A review of materials and their applications. *Journal of Materiomics*, *4*(2), 108-120.

Meng, X., Kwon, T. Y., Yang, Y., Ong, J. L., & Kim, K. H. (2006). Effects of applied voltages on hydroxyapatite coating of titanium by electrophoretic deposition. *Journal of Biomedical Materials Research Part B: Applied Biomaterials: An Official Journal of The Society for Biomaterials, The Japanese Society for Biomaterials, and The Australian Society for Biomaterials and the Korean Society for Biomaterials*, *78*(2), 373-377.

Michael, J. R. (2011). High resolution at low beam energy in the SEM: resolution measurement of a monochromated SEM. *Scanning*, *33*(3), 147-154.

Mondragon-Cortez, P., & Vargas-Gutierrez, G. (2004). Electrophoretic deposition of hydroxyapatite submicron particles at high voltages. *Materials Letters*, *58*(7-8), 1336-1339.

Mouritz, A. P. (2012). *Introduction to aerospace materials*. London:Elsevier.

Muñoz, A., & Costa, M. (2012). Elucidating the mechanisms of nickel compound uptake: a review of particulate and nano-nickel endocytosis and toxicity. *Toxicology and applied pharmacology*, *260*(1), 1-16.

Murugan, R., & Ramakrishna, S. (2005). Development of nanocomposites for bone grafting. *Composites science and technology*, *65*(15-16), 2385-2406.

Niinomi, M. (2019). *Metals for biomedical devices*. Cambridge:Woodhead publishing.

Nyamukamba, P., Okoh, O., Mungondori, H., Taziwa, R., & Zinya, S. (2018). Synthetic Methods for Titanium Dioxide Nanoparticles: A Review *Titanium Dioxide-Material for a Sustainable Environment*: IntechOpen.

Ojeda, J. J., & Dittrich, M. (2012). Fourier transform infrared spectroscopy for molecular analysis of microbial cells *Microbial Systems Biology*, *38* (5), 187-211.

Park, B., & Kim, Y. K. (2003). *Metallic biomaterials*. Berlin:Springer.

Park, J., & Lakes, R. S. (2007). *Biomaterials: an introduction*. Berlin:Springer.

Paunovic, M. (2007). Electrochemical deposition. *Encyclopedia of Electrochemistry: Online* 57, 126-138.

Paunovic, M., & Schlesinger, M. (2006). *Fundamentals of electrochemical deposition*. New Jersey: John wiley & sons.

Pichugin, V. F., Surmenev, R. A., Shesterikov, E. V., Ryabtseva, M., Eshenko, E., Tverdokhlebov, S. I., Epple, M. (2008). The preparation of calcium phosphate coatings on titanium and nickel–titanium by rf-magnetron-sputtered deposition: composition, structure and micromechanical properties. *Surface and Coatings Technology*, *202*(16), 3913-3920.

Pierson, H. O. (1996). *Handbook of refractory carbides and nitrides*: p*roperties, characteristics, processing and applications*. New York:William Andrew.

Powers, R. (1975). The electrophoretic forming of beta-alumina ceramic. *Journal of The Electrochemical Society*, *122*(4), 490-500.

Ramakrishna, S., Mayer, J., Wintermantel, E., & Leong, K. W. (2001). Biomedical applications of polymer-composite materials: a review. *Composites Science and Technology*, *61*(9), 1189-1224.

Roy, M., Bandyopadhyay, A., & Bose, S. (2011). Induction plasma sprayed nano hydroxyapatite coatings on titanium for orthopaedic and dental implants. *Surface and Coatings Technology*, *205*(8-9), 2785-2792.

Rößler, S., Sewing, A., Stölzel, M., Born, R., Scharnweber, D., Dard, M., & Worch, H. (2003). Electrochemically assisted deposition of thin calcium phosphate coatings at near-physiological pH and temperature. *Journal of Biomedical Materials Research*, *64*(4), 655-663.

Samavedi, S., Whittington, A. R., & Goldstein, A. S. (2013). Calcium phosphate ceramics in bone tissue engineering: a review of properties and their influence on cell behavior. *Acta biomaterialia*, *9*(9), 8037-8045.

Seuss, S., & Boccaccini, A. R. (2013). Electrophoretic deposition of biological macromolecules, drugs, and cells. *Biomacromolecules*, *14*(10), 3355-3369.

Shadanbaz, S., & Dias, G. J. (2012). Calcium phosphate coatings on magnesium alloys for biomedical applications: a review. *Acta Biomaterialia*, *8*(1), 20-30.

Surmenev, R. A. (2012). A review of plasma-assisted methods for calcium phosphate-based coatings fabrication. *Surface and Coatings Technology*, *206*(8-9), 2035-2056.

Thamaraiselvi, T., & Rajeswari, S. (2004). Biological evaluation of bioceramic materials-a review. *Carbon*, *24* (31), 172.

Wang, L., & Nancollas, G. H. (2008). Calcium orthophosphates: crystallization and dissolution. *Chemical reviews*, *108* (11), 4628-4669.

Wang, Y. C., Leu, I. C., & Hon, M. H. (2004). Kinetics of electrophoretic deposition for nanocrystalline zinc oxide coatings. *Journal of the American Ceramic Society*, *87* (1), 84-88.

Wei, M., Ruys, A., Milthorpe, B., & Sorrell, C. (2005). Precipitation of hydroxyapatite nanoparticles: effects of precipitation method on electrophoretic deposition. *Journal of Materials Science: Materials in Medicine*, *16*(4), 319-324.

Wei, M., Ruys, A., Swain, M., Kim, S., Milthorpe, B., & Sorrell, C. (1999). Interfacial bond strength of electrophoretically deposited hydroxyapatite coatings on metals. *Journal of Materials Science: Materials in Medicine*, *10* (7), 401-409.

Wenz, H. J., Bartsch, J., Wolfart, S., & Kern, M. (2008). Osseointegration and clinical success of zirconia dental implants: a systematic review. *International Journal of Prosthodontics*, *21* (1) 27-36.

Wiederhorn, S., & Bolz, L. (1970). Stress corrosion and static fatigue of glass. *Journal of the American Ceramic Society*, *53* (10), 543-548.

Xiao, X. F., & Liu, R. F. (2006). Effect of suspension stability on electrophoretic deposition of hydroxyapatite coatings. *Materials Letters*, *60*(21-22), 2627-2632.

Yang, Y.-C., & Yang, C.-Y. (2013). Mechanical and histological evaluation of a plasma sprayed hydroxyapatite coating on a titanium bond coat. *Ceramics International*, *39*(6), 6509-6516.

Yi, C. P., & Majid, S. R. (2018). The Electrochemical Performance of Deposited Manganese Oxide-Based Film as Electrode Material for Electrochemical Capacitor Application *Semiconductors-Growth and Characterization*. London:InTech.

Yin, X., Stott, M., & Rubio, A. (2003). α-and β-tricalcium phosphate: A density functional study. *Physical Review B, 68* (20), 201-205.

Zavan, B. (2017). Biocompatibility and cellular response to dental implant materials *Bone Response to Dental Implant Materials*, 25, 211-227.

Zeng, H., & Lacefield, W. R. (2000). The study of surface transformation of pulsed laser deposited hydroxyapatite coatings. *Journal of Biomedical Materials Research*, *50* (2), 239-247.

Zhitomirsky, I. (1998). Electrophoretic and electrolytic deposition of ceramic coatings on carbon fibers. *Journal of the European Ceramic Society*, *18* (7), 849-856.

Zhitomirsky, I. (2002). Cathodic electrodeposition of ceramic and organoceramic materials. Fundamental aspects. *Advances in Colloid and Interface Science, 97* (1-3), 279-317.

Zhitomirsky, I., & Gal-Or, L. (1997). Electrophoretic deposition of hydroxyapatite. *Journal of Materials Science*: *Materials in Medicine, 8* (4), 213-219.

Zhou, J., Sun, Y., Huang, S., Sheng, J., Li, J., & Agyenim-Boateng, E. (2019). Effect of laser peening on friction and wear behavior of medical Ti6Al4V alloy. *Optics & Laser Technology*, *109*, 263-269.